

NASA TM X-55428

# EGO ORBITAL PARAMETERS AND HEAT INPUTS

GPO PRICE \$ \_\_\_\_\_

CFSTI PRICE(S) \$ \_\_\_\_\_

Hard copy (HC) 3.00

Microfiche (MF) .75

7 653 July 65

BY  
**H. E. MONTGOMERY  
AND  
S. J. PADDACK**

N66-21006

FACILITY FORM 808

(ACCESSION NUMBER)	(THRU)
<u>79</u>	<u>1</u>
(PAGES)	(CODE)
	<u>30</u>
(NASA CR OR TMX OR AD NUMBER)	(CATEGORY)

APRIL 1, 1963



**GODDARD SPACE FLIGHT CENTER**  
GREENBELT, MD.

807-36524

EGO ORBITAL PARAMETERS  
AND HEAT INPUTS

by

H. E. Montgomery

S. J. Paddack

Special Projects Branch  
Theoretical Division

National Aeronautics and Space Administration  
Goddard Space Flight Center  
Greenbelt, Maryland

TABLE OF CONTENTS

I.	Introduction . . . . .	1
II.	Nomenclature . . . . .	2
III.	Assumptions . . . . .	10
	A. Injection Conditions . . . . .	10
	B. Restraints on Launch Time . . . . .	10
IV.	Mathematical Model . . . . .	10
	A. Ideal Control Laws and Definition of Coordinate Systems ..	10
	B. Development of Position and Velocity Vectors . . . . .	13
	1. Earth-Sun Vector, $\bar{r}_{SE}$ . . . . .	13
	2. Earth-Vehicle Vector, $\bar{r}_{VE}$ . . . . .	16
	3. Earth-Vehicle Velocity Vector, $\dot{\bar{r}}_{VE}$ . . . . .	17
	4. Vehicle-Sun Vector, $\bar{r}_{SV}$ . . . . .	18
	C. Orbital Parameters and Spacecraft Angles . . . . .	13
	1. True Anomaly, $\nu$ . . . . .	18
	2. Solar Array Angle, $\varphi_p$ . . . . .	19
	3. OPEP Angle, $\gamma_e$ . . . . .	19
	4. Angle Between the Line of Apsides and the Ecliptic Plane, $\Psi$ . . . . .	20
	5. Flight Path Angle, $\gamma$ . . . . .	21
	6. OPEP - Velocity Vector Angle, $\theta_e$ . . . . .	21
	7. Angle Between the Projection of the Line of Apsides On The Ecliptic Plane and the Earth-Sun Line, $\xi$ . . . . .	21
	8. The Distance From the Center of the Earth to the Satellite, $r_{VE}$ . . . . .	22
	D. Heat Inputs to an Arbitrarily Oriented Surface of EGO . . . . .	22
	1. Earth Emitted Radiant Heat . . . . .	22
	2. Direct Solar Radiant Heat . . . . .	25
	3. Reflected Solar Radiant Heat . . . . .	26
V.	Computer Programs . . . . .	28
	A. The Launch Window Program . . . . .	28
	B. The Interplanetary Trajectory Program . . . . .	29

VI. Results and Discussion . . . . .	30
A. Orbital Parameters and Spacecraft Angles . . . . .	30
1. True Anomaly, $v$ . . . . .	31
2. Solar Array Angle, $\alpha_p$ . . . . .	31
3. OPEP Angle, $\psi_e$ . . . . .	31
4. Angle Between The Line of Apsides and the Ecliptic Plane, $\psi$ . . . . .	31
5. Flight Path Angle, $\gamma$ . . . . .	32
6. OPEP - Velocity Vector Angle, $\theta_e$ . . . . .	32
7. Angle Between the Projection of The Line of Apsides on the Ecliptic Plane and the Earth-Sun Line, $\xi$ . . . . .	32
8. The Distance From the Center of the Earth to The Satellite, $r_{VE}$ . . . . .	33
B. Heat Inputs to EGO . . . . .	33
1. Main Box . . . . .	
a. Earth Emitted . . . . .	34
b. Direct Solar . . . . .	34
c. Reflected Solar . . . . .	34
2. Solar Array . . . . .	35
a. Earth Emitted . . . . .	35
b. Direct Solar . . . . .	35
c. Reflected Solar . . . . .	36
3. Orbit Plane Experiment Package (OPEP) . . . . .	36
a. Earth Emitted . . . . .	36
b. Direct Solar . . . . .	36
c. Reflected Solar . . . . .	37
VII. Conclusions . . . . .	38
VIII. References . . . . .	39

## LIST OF FIGURES

- Figure 1. Body Coordinate System.
- Figure 2. Geometry of the elliptic two-body orbit.
- Figure 3. Geometry for heat inputs.
- Figure 4. Geometry for Earth emitted heat inputs.  
Case 1. Satellite surface with unit normal  $\bar{n}$  cannot see the Earth.
- Figure 5. Geometry for Earth emitted heat inputs.  
Case 2. Satellite surface with unit normal  $\bar{n}$  can see a portion of the Earth's surface within the tangent cone.
- Figure 6. Geometry for Earth emitted heat inputs.  
Case 3. Satellite surface with unit normal  $\bar{n}$  can see the entire surface of the Earth within the tangent cone.
- Figure 7. Comparison between actual and approximate solar reflected heat inputs.
- Figure 8. Geometry for reflected solar heat inputs.
- Figure 9. True anomaly vs. time from perigee.
- Figure 10. Solar array angle vs. time from perigee.
- Figure 11. OPEP angle vs. time from perigee.
- Figure 12. Angle between line of apsides and the ecliptic plane vs. time from injection.
- Figure 13. Flight path angle vs. time from perigee
- Figure 14. OPEP-velocity vector angle vs. time from perigee.
- Figure 15. Angle between the projection of the line of apsides on the ecliptic plane and the Earth-Sun line vs. time.
- Figure 16. The distance from the center of the Earth to the satellite vs. time from perigee.

- Figure 17. Earth emitted heat inputs to main box vs. time from perigee.
- Figure 18. Direct solar heat inputs to main box vs. time from perigee.
- Figure 19. Reflected solar heat inputs to main box vs. time from perigee.
- Figure 20. Earth emitted heat inputs to solar array vs. time from perigee.
- Figure 21. Direct solar heat inputs to solar array vs. time from perigee.
- Figure 22. Reflected solar heat inputs to solar array vs. time from perigee.
- Figure 23. Earth emitted heat inputs to OPEP vs. time from perigee.
- Figure 24. Direct solar heat inputs to OPEP vs. time from perigee.
- Figure 25. Reflected solar heat inputs to OPEP vs. time from perigee.

EGO ORBITAL PARAMETERS  
AND HEAT INPUTS

by

H. E. Montgomery  
S. J. Paddack

Special Projects Branch  
Theoretical Division  
Goddard Space Flight Center  
Greenbelt, Maryland

SUMMARY

The Orbiting Geophysical Observatory (OGO) is an actively oriented satellite which will carry up to fifty experiments. The experiments will be oriented relative to the Sun, Earth or the orbit plane. This document presents methods of analysis for computing orbital data, spacecraft angle data and spacecraft heat input data for OGO, and gives specific results for the S-49, Eccentric Orbiting Geophysical Observatory (EGO). The orbital data include the transient behavior of true anomaly, the flight path angle, the distance from the center of the Earth to the satellite, the angle between the line of apsides and the ecliptic plane, and the angle between the projection of the line of apsides on the ecliptic plane and the Earth-Sun line. The spacecraft angle data include the transient behavior of solar array angle, the orbital plane experiment package (OPEP) angle and the OPEP velocity vector angle. The transient heat input data include Earth emitted heat, direct solar heat and Earth reflected solar heat inputs to all the faces of the main OGO box, the solar array and the OPEP.

EGO ORBITAL PARAMETERS  
AND HEAT INPUTS

by

H. E. Montgomery  
S. J. Paddack

Special Projects Branch  
Theoretical Division  
Goddard Space Flight Center  
Greenbelt, Maryland

I. INTRODUCTION

This report presents orbital data, spacecraft angle data and heat input data for EGO. A detailed description of the methods used in the calculations is also given. The calculated results are consistent with the "EGO Launch Window Study", NASA Report Number X643-62-225 (Reference 1), insofar as the perigee restraint is concerned. A slightly different set of initial conditions was used in Reference 1, but the launch window map will still give a good estimate of launch times consistent with the perigee restraint. The data presented in this report are for launch times for which the perigee will not go below its initial value for a whole year. The injection parameters for this report were taken from Reference 2.

## II. NOMENCLATURE

- $A_c$  = Azimuth = the compass heading measured clockwise from north.
- $a$  = The semi-major axis of the satellite's orbit.
- $a'$  = 1 A.U. =  $1.496 \times 10^8$  kilometers = the semi-major axis of the Sun's orbit relative to the Earth (Reference 6).
- $C$  =  $(\bar{i}_b \times \bar{i}_e) \cdot \bar{k}_b$  by definition.
- $d$  = The number of days from 0.0 hours Universal Time on January 1, 1961 to the time in question.
- $dA$  = An elemental area of the Earth's surface. (See Figure 3).
- $E$  = The satellite's eccentric anomaly.
- $e$  = The eccentricity of the satellite's orbit.
- $e'$  = 0.0167259 = the eccentricity of the Sun's orbit relative to the Earth. (Page 50 of Reference 7).
- $F_a$   $\equiv \frac{q_a}{\sigma S}$  = the reflected solar radiation factor.
- $F_E$   $\equiv \frac{q_E}{\Lambda}$  = the Earth emitted radiation factor.
- $F_S$   $\equiv \frac{q_S}{S} \approx \frac{\bar{n} \cdot \bar{r}_{SV}}{|\bar{r}_{SV}|}$  = the direct solar factor.
- $f_a(\eta, \mu, \beta, \rho)$  = The integrand of the integral for  $q_a$ . (See page 26 )

## NOMENCLATURE (Cont)

- $f_E(\eta, \mu, \rho)$  = The integrand of the integral for  $q_E$ . (See page 23.)
- $G M_E$  =  $3.986032 (\pm 0.000030) \times 10^5 \text{ km}^3 \text{ sec}^{-2}$  =  
the gravitational constant of the Earth.  
(Reference 6).
- $g'$  = Mean anomaly of the Sun relative to the Earth.
- $H$  =  $\frac{r_{VE}}{R_e}$ .
- $\bar{H}_m$  =  $\bar{r}_{VE} \times \dot{\bar{r}}_{VE}$  = The angular momentum vector.
- $h$  = Height = the distance from the reference sphere  
(of radius equal to the Earth's equatorial radius)  
to the spacecraft measured along the geocentric  
radius vector.
- $i$  = Inclination = the angle between the satellite's orbit  
plane and the equatorial plane.
- $\bar{i}, \bar{j}, \bar{k}$  = The unit vectors which correspond to X, Y and Z, respectively.
- $\bar{i}_b, \bar{j}_b, \bar{k}_b$  = The unit vectors which correspond to  $x_b, y_b,$  and  $z_b,$   
respectively. (See Figure 1).
- $\bar{i}_e, \bar{j}_e, \bar{k}_e$  = The unit vectors which correspond to the  $x_e, y_e,$  and  $z_e$   
coordinates, respectively. (See Figure 1).
- $\bar{i}_p, \bar{j}_p, \bar{k}_p$  = The unit vectors which correspond to  $x_p, y_p,$  and  $z_p,$   
respectively. (See Figure 1).

## NOMENCLATURE (Cont)

- $\bar{k}'$  = The unit vector which is normal to the ecliptic plane and points north.
- $L'$  =  $w' + g'$  = the mean longitude of the Sun.
- $\bar{n}$  = The unit outward normal of the surface in question.
- $\bar{P}, \bar{Q}, \bar{R}$  = The unit vectors which correspond to  $x_w, y_w,$  and  $z_w,$  respectively. (See Figure 2).
- $P_X, P_Y, P_Z$  = The components of the  $\bar{P}$  unit vector in the (X, Y, Z) system.
- $Q_X, Q_Y, Q_Z$  = The components of the  $\bar{Q}$  unit vector in the (X, Y, Z) system.
- $q_a$  = The heat flux, incident upon the flat surface, which originates at the Sun and reflects from the Earth to the vehicle.
- $q_E$  = The heat flux, incident upon the flat surface, which radiates from the Earth.
- $q_S$  = The heat flux, incident upon the flat surface in question, whose source is the Sun.
- $R_e$  = The equatorial radius of the Earth.
- $R_X, R_Y, R_Z$  = The components of the  $\bar{R}$  unit vector in the (X, Y, Z) system.

## NOMENCLATURE (Cont)

- $\bar{r}_{SE}$  = The position vector which points from the center of the Earth to the Sun.
- $\bar{r}_{VE}$  = The position vector from the Earth to the vehicle.
- $\dot{\bar{r}}_{VE}$  = The velocity of the satellite relative to the Earth.
- $\bar{r}_{VS}$  = The position vector which points from the Sun to the vehicle.
- S =  $1.97 \pm 0.01 \text{ cal cm}^{-2} \text{ minutes}^{-1} = 0.1374 \text{ watt. cm}^{-2}$   
= Flux of total radiation received outside Earth's atmosphere per unit area at mean Sun-Earth distance. (Reference 12).
- $\bar{u}_{SE}$  =  $\frac{\bar{r}_{SE}}{|\bar{r}_{SE}|}$  = The unit vector which points from the center of the Earth to the Sun.
- $v_s$  = The speed of the vehicle.
- X, Y, Z = Cartesian coordinates with the origin at the center of the Earth, the X-axis in the direction of the vernal equinox, the Z-axis along the north pole of the Earth, and the Y-axis forms a right hand set.
- $x_b, y_b, z_b$  = This coordinate system is fixed to the main OGO box. (Figure 1).
- $x_e, y_e, z_e$  = The OPEP coordinates and are defined with respect to the  $(x_b, y_b, z_b)$  system by the OPEP angle  $\psi_e$ . (Figure 1).

## NOMENCLATURE (Cont)

- $x_p, y_p, z_p$  = The paddle coordinates and are defined with respect to the  $(x_b, y_b, z_b)$  system by the paddle angle  $\varphi_p$ . (Figure 1).
- $x_w, y_w, z_w$  = Cartesian coordinates with the origin at the center of the Earth, the  $x_w$  - axis is in the direction of perigee, the  $y_w$  - axis is advanced  $90^\circ$  in the direction of motion, and the  $z_w$  - axis is in the direction of the satellite's angular momentum vector. (Figure 2).
- $\alpha$  = The albedo = the fraction of the solar constant  $S$  which is reflected away from the Earth. The value for  $\alpha$  is about 0.34. (Reference 12).
- $\beta$  = The angle between the vector  $\bar{u}_{SE}$  which points from the center of the Earth to the Sun and the outward-directed normal of the Earth's elemental surface area  $dA$ . (Figure 3).
- $\gamma$  = Flight path angle = the angle between the velocity vector and the plane normal to the radius vector passing through the vehicle.
- $\delta$  =  $\varphi_p - 90^\circ$  by definition.
- $\epsilon$  = The angle between the equatorial plane and the ecliptic plane.
- $\eta$  = The angle between the outward-directed normal of  $dA$  and the vector  $\bar{\rho}$ . (Figure 3).

$\theta$  = . Terrestrial longitude = the angular distance from the Greenwich meridian, measured eastward along the equator to the meridian plane of the vehicle.

$\theta_e$  = OPEP - velocity vector angle = the angle between the vectors  $\bar{i}_e$  and  $\dot{\bar{r}}_{VE}$ .

$\theta_S$   $\equiv \frac{\bar{u}_{SE} \cdot \bar{r}_{VE}}{|\bar{r}_{VE}|}$  , (Figure 3).

$\Lambda$  = 0.02215 watts  $\text{cm}^{-2}$  = the emittance per unit area of the surface of the Earth.

$\lambda$  =  $\cos^{-1} \left( - \frac{\bar{r}_{VE}}{|\bar{r}_{VE}|} \cdot \bar{n} \right)$  = the angle between the vector  $-\bar{r}_{VE}$  and the unit vector  $\bar{n}$ . (Figure 3)

$\lambda'$  =  $\nu' + \omega'$  = True longitude of the Sun = the angle between the positive X-axis (Vernal Equinox) and the vector which points from the Earth to the Sun  $\bar{r}_{SE}$ . It is measured in the direction of motion from the X-axis.

$\mu$  = The angle between the outward-directed normal of the plate  $\bar{n}$  and the vector  $(-\bar{\rho})$ . (Figure 3).

$\nu$  = The satellite's true anomaly.

$\nu'$  = True anomaly of the Sun = the angle between the vector which points from the center of the Earth to the Sun's perigee and the vector which points from the center of the Earth to the Sun. It is measured in the direction of motion of the Sun.

NOMENCLATURE (Cont)

- $\xi$  = The angle between the projection of the  $(-\bar{P})$  on the ecliptic plane and  $\bar{r}_{SE}$ .
- $\bar{p}$  = The vector which points from the Earth's elemental area  $dA$  to the vehicle. (See Figure 3).
- $\sigma$  =  $5.735 \times 10^{-12}$  watt  $\text{cm}^{-2}$   $^{\circ}\text{K}^{-4}$  = the Stephan-Boltzman constant.
- $\tau$  = Time from the injection into orbit.
- $\phi$  = Geocentric latitude = the angle at the center of the Earth between the radius through a given point and the equatorial plane.
- $\phi_c$  = The angle between the plane formed by the vector  $\bar{r}_{VE}$  and  $\bar{r}_{SE}$ ; and the plane formed by the vector  $\bar{r}_{VE}$  and  $\bar{n}$ . (Figure 8).
- $\phi_H$  =  $\sin^{-1} \left( \frac{1}{H} \right)$  = the maximum look angle for which the satellite can see the surface of the Earth. (Figure 4).
- $\phi_p$  = The solar array angle = the angle measured counter clockwise from the  $\bar{j}_b$  vector to the  $\bar{j}_p$  vector when observed from the positive end of the  $\bar{i}_b$  vector. (Figure 1).
- $\gamma$  = The minimum angle between the vector pointing from the center of the Earth to apogee and the ecliptic plane.

## NOMENCLATURE (Cont)

- $\psi_e$  = The OPEP angle = the angle measured counter clockwise from the vector  $\bar{i}_b$  to the vector  $\bar{i}_e$ , when observed from the positive end of the vector  $\bar{k}_b$ .
- $\Omega$  = Longitude of the ascending node = the angular distance from the vernal equinox measured eastward in the equatorial plane to the point of intersection of the orbit plane where the satellite crosses from south to north.
- $\omega$  = The argument of perigee = the angular distance measured in the orbital plane from the line of nodes to the line of apsides.
- $\omega'$  = The argument of perigee of the Sun = the angle between the positive X-axis (Vernal Equinox) and the vector from the center of the Earth to the Sun's perigee measured in the direction of motion from the X-axis.
- $\dot{\Omega}$  = The time rate of change of  $\Omega$ .
- $\dot{\omega}$  = The time rate of change of  $\omega$ .

### III. ASSUMPTIONS

#### A. INITIAL CONDITIONS

The initial conditions are assumed to be the same as the Agena burnout conditions (Reference 2) namely:

$\phi$	=	-20.280	degrees = geocentric latitude
$\theta$	=	111.902	degrees = terrestrial longitude
$h$	=	281621.6	meters = geocentric height
$v_s$	=	10645.27	meters per second = the speed of the vehicle
$A_c$	=	66.355	degrees = azimuth
$\gamma$	=	1.47148	degrees = flight path angle

#### B. RESTRAINTS ON LAUNCH TIME

For the purpose of generating results for this report the only restraint on launch time is the one on perigee latitude. This restraint states that the perigee altitude will not go below its initial value for one year. The allowable launch times were chosen from the launch window map in Reference 1. A slightly different set of initial conditions was used in Reference 1, but the launch window map gives a good estimate of launch times consistent with the perigee restraint.

### IV. MATHEMATICAL MODEL

#### A. IDEAL CONTROL LAWS AND DEFINITION OF COORDINATE SYSTEMS

Figure 1 presents the body coordinate systems. The  $x_b, y_b, z_b$  coordinate system is fixed to the main box. The solar paddle coordinate system  $x_p, y_p, z_p$  is defined with respect to the

$x_b, y_b, z_b$  system by the paddle angle  $\psi_p$ . The  $y_p$  axis is the outward-directed normal to the surface of the paddle which bears the solar cells. The OPEP (Orbit Plane Experiment Package) coordinate system  $x_e, y_e, z_e$  is defined with respect to the  $x_b, y_b, z_b$  system by the OPEP angle  $\psi_e$ . The  $x_e$  axis is the outward-directed normal of the surface of the OPEP which is facing in the direction of motion.

It is assumed that the OGO spacecrafts obey ideal control laws.

A definition of these control laws follows:

1. The  $+z_b$  - face will be aligned with radius vector from the center of the Earth to the satellite. (Page 23 of Reference 3).

In equation form this states that

$$\bar{k}_b = - \frac{\bar{r}_{VE}}{|\bar{r}_{VE}|}$$

2. The solar array ( $x_p-z_p$  plane) will be normal to the vector from the Sun to the satellite. In equation form this states that

$$\bar{j}_p = - \frac{\bar{r}_{VS}}{|\bar{r}_{VS}|}$$

3. The Sun will not shine on the + y<sub>b</sub> - face of the main box  
 (Page 20 of Reference 4). In equation form this states that

$$\bar{r}_{VS} \cdot \bar{j}_b = \bar{r}_{VS} \cdot (\bar{k}_b \times \bar{i}_b) \geq 0$$

4. The positive x<sub>e</sub> - face of the orbit plane experiment  
 package (OPEP) shall look forward in the plane of the orbit.  
 (Page 24 of reference 3). In equation form this states that

$$\dot{\bar{r}}_{VE} \cdot \bar{i}_e \geq 0$$

and

$$\bar{i}_e = \frac{\bar{k}_b \times \bar{H}_m}{|\bar{k}_b \times \bar{H}_m|}$$

Where  $\bar{H}_m = \bar{r}_{VE} \times \dot{\bar{r}}_{VE}$  is the angular momentum vector. With these four control laws three orthogonal coordinate systems may be established; box ( $\bar{i}_b, \bar{j}_b, \bar{k}_b$ ), solar array ( $\bar{i}_s, \bar{j}_s, \bar{k}_s$ ) and OPEP ( $\bar{i}_e, \bar{j}_e, \bar{k}_e$ ). The vectors  $\bar{k}_b$  and  $\bar{j}_p$  are obtained directly from laws 1 and 2 respectively. Since  $\bar{i}_b$  is perpendicular to both  $\bar{j}_p$  and  $\bar{k}_b$  it follows that

$$\bar{i}_b = \pm \frac{\bar{k}_b \times \bar{j}_p}{|\bar{k}_b \times \bar{j}_p|}$$

The sign of the expression for  $\bar{i}_b$  is determined from control law number 3. The vector  $\bar{j}_b$  is determined from  $\bar{j}_b = \bar{k}_b \times \bar{i}_b$ . By construction  $\bar{k}_e = \bar{k}_b$ . Also, by construction  $\bar{i}_p = \bar{i}_b$ . Then it follows that  $\bar{k}_p = \bar{j}_p \times \bar{i}_p$ . The vector  $\bar{i}_e$  is determined by control law number 4, and lastly,  $\bar{j}_e = \bar{k}_e \times \bar{i}_e$ .

## B. DEVELOPMENT OF POSITION AND VELOCITY VECTORS.

### 1. Earth-Sun Vector $\bar{r}_{SE}$ --

This is the vector which points from the center of the Earth to the center of the Sun.

$$\bar{r}_{SE} = r_{SE} \bar{u}_{SE}$$

where  $r_{SE}$  is the magnitude of  $\bar{r}_{SE}$ , and  $\bar{u}_{SE}$  is the unit vector which points from the center of the Earth to the center of the Sun. The value of  $r_{SE}$  may be calculated with the expression (page 164 of Reference 5)

$$r_{SE} = \frac{a' (1 - e'^2)}{1 + e' \cos \nu'}$$

where

$a' = 1 \text{ a.u.} = 1.49599 \times 10^8 \text{ kilometers} = \text{the semi-major axis of the Sun's orbit relative to the Earth. (Reference 6).}$

$e' = 0.0167259 = \text{the eccentricity of the Sun's orbit relative to the Earth. (page 50 of Reference 7).}$

$v' = \text{the true anomaly of the Sun relative to the Earth}$   
 $\approx g' + 2 e' \sin g' , \text{ since } e' \text{ is small. (page 171 of Reference 5).}$

$g' = -3.2419100 \times 10^{-2} + 1.7201970 \times 10^{-2} d = \text{the mean anomaly of the Sun relative to the Earth. (Page 498 of Reference 7).}$

$d = \text{the number of days from 0.0 hours Universal Time on 1 January, 1961. (Page 498 of Reference 7).}$

The unit vector  $\bar{u}_{SE}$  is given by

$$\bar{u}_{SE} = \bar{i} \cos \lambda' + \bar{j} \cos e \sin \lambda' + \bar{k} \sin e \sin \lambda'$$

where

$\epsilon$  = The angle between the equatorial plane and the ecliptic plane.

$\lambda'$  = True longitude of the Sun.

$$= \omega' + \lambda' \approx \omega' + g' + 2e \sin g' = L' + 2e \sin g'$$

$$\approx 4.894 117 + 0.017202791 d$$

$$+ 0.03345099 \sin \left[ -0.0324191 + 0.01720197 d \right]$$

$\omega'$  = Argument of perigee

$L' = \omega' + g' =$  Mean longitude of the Sun.

A more convenient form for the unit vector  $\bar{u}_{SE}$  is

$$\bar{u}_{SE} = (\bar{u}_{SE} \cdot \bar{P}) \bar{P} + (\bar{u}_{SE} \cdot \bar{Q}) \bar{Q} + (\bar{u}_{SE} \cdot \bar{R}) \bar{R}$$

$$\bar{u}_{SE} = (P_X \cos \lambda' + P_Y \cos \epsilon \sin \lambda' + P_Z \sin \epsilon \sin \lambda') \bar{P}$$

$$+ (Q_X \cos \lambda' + Q_Y \cos \epsilon \sin \lambda' + Q_Z \sin \epsilon \sin \lambda') \bar{Q}$$

$$+ (R_X \cos \lambda' + R_Y \cos \epsilon \sin \lambda' + R_Z \sin \epsilon \sin \lambda') \bar{R}$$

where

$P_X, P_Y, P_Z$  are the components of the unit vector  $\bar{P}$

$Q_X, Q_Y, Q_Z$  are the components of the unit vector  $\bar{Q}$

$R_X, R_Y, R_Z$  are the components of the unit vector  $\bar{R}$

## 2. Earth-Vehicle Vector $\bar{r}_{VE}$

The vector  $\bar{r}_{VE}$  points from the center of the Earth to the vehicle. The Launch Window Program cannot be used to calculate the vector  $\bar{r}_{VE}$  as a function of time for tracking purposes. It can, however, give an adequate estimate of the vector  $\bar{r}_{VE}$  relative to other vectors

$\bar{r}_{SE}, \bar{r}_{SV}, \bar{i}_b, \bar{j}_b, \bar{k}_b, \bar{i}_p, \bar{j}_p, \bar{k}_p, \bar{i}_e, \bar{j}_e, \bar{k}_e, \text{ etc } \dots$

as a function of time from perigee.

It is assumed that at any particular time  $\tau$  for which the Launch Window Program has calculated the orbital elements ( $a, e, i, \omega, \Omega$ ), the satellite is at perigee. At times subsequent to  $\tau$ , up to one orbital period, two body motion is assumed. The position vector may be written in the form (Pages 54 and 65 of Reference 8)

$$\bar{r}_{VE} = \bar{P}a(\cos E - e) + \bar{Q}e\sqrt{1-e^2}\sin E$$

where,

- a = The semi-major axis of the satellite's orbit
- E = The eccentric anomaly of the satellite's orbit
- e = The eccentricity of the satellite's orbit
- $\bar{P}$  = The unit vector which points from the center of the Earth to the satellite's perigee
- $\bar{Q}$  = The unit vector which is rotated  $90^\circ$  in the plane of the satellite's orbit in the direction of motion.

These assumptions can be made since the relative locations of the Sun and the Earth with respect to the orbit do not change enough in one EGO period to be seen as a first order effect on any of the parameters presented in this report.

The errors in orbit shape and orientation are allowed to accumulate for only one orbital period, since the orbit is rectified after each period. The Sun moves approximately one degree per day relative to the Earth; the orbit plane precesses about 0.65 degrees per day; and the line of apsides moves in the orbit plane about 0.85 degrees per day, therefore, the errors are small.

### 3. The Vehicle Velocity Vector $\dot{\bar{r}}_{VE}$

The same assumptions are made for the velocity vector of the vehicle relative to the Earth as in the case of the vector  $\bar{r}_{VE}$ . The vector  $\dot{\bar{r}}_{VE}$  may be written as (Page 282 of Reference 8)

$$\dot{\bar{r}}_{VE} = \frac{1}{r_{VE}} \left( -\bar{P} \sqrt{a GM_E} \sin E + \bar{Q} \sqrt{a GM_E (1-e^2)} \cos E \right)$$

where,

$$GM_E = 3.986032 \times 10^5 \text{ km}^3 \cdot \text{sec}^{-2} =$$

#### 4. The Satellite-Sun Vector $\bar{r}_{SV}$

The vector which points from the satellite to the Sun is

$$\bar{r}_{SV} = \bar{r}_{SE} - \bar{r}_{VE}$$

The vectors  $\bar{r}_{SE}$  and  $\bar{r}_{VE}$  are given in sections 1 and 2 above.

### C. ORBITAL PARAMETERS AND SPACECRAFT ANGLES

#### 1. True Anomaly $v$

The true anomaly,  $v$ ,

is the angle between the vector from the center of the Earth to perigee and the vector from the center of the Earth to the satellite measured from the perifocus in the direction of motion. (See Figure 2).

The following formulas were selected to calculate  $v$  (Page 341, Reference 9):

$$\cos v = \frac{\cos E - e}{1 - e \cos E}$$

and

$$\sin v = \frac{\sqrt{1-e^2} \sin E}{1 - e \cos E}$$

## 2. Solar Array $\varphi_p$

The angle measured counter-clockwise from the  $\bar{j}_b$  vector to  $\bar{j}_p$  vector when observed from the positive end of the  $\bar{i}_b$  vector is defined as the solar array angle,  $\varphi_p$ . (See Figure 1). Consistent with this notation the planned range for the variation of  $\varphi_p$  for OGO is  $90^\circ \leq \varphi_p \leq 270^\circ$ . (Page 20, Reference 4).  $\delta$  is the angle between the  $\bar{j}_p$  vector and the  $\bar{k}_b$  vector measured counter-clockwise from  $\bar{k}_b$  when observed from the positive end of the  $\bar{i}_b$  vector. It follows that when  $\varphi_p$  goes from  $90^\circ$  to  $270^\circ$ ,  $\delta$  goes from  $0^\circ$  to  $180^\circ$ . Therefore,  $\varphi_p = \delta + 90^\circ$  and  $\cos \delta = \bar{j}_p \cdot \bar{k}_b$ . Therefore,  $\varphi_p$  may be found from the formula

$$\varphi_p = \cos^{-1} (\bar{j}_p \cdot \bar{k}_b) + 90^\circ$$

where

$$0^\circ \leq \cos^{-1} (\bar{j}_p \cdot \bar{k}_b) \leq 180^\circ$$

## 3. OPEP Angle $\psi_e$

This angle is measured counter-clockwise from the vector  $\bar{i}_b$  to the vector  $\bar{i}_e$  when observed from the positive end of the vector  $\bar{k}_b$ . (See Figure 1). The OPEP control system is designed such that the range for the OPEP angle is  $\pm 225^\circ$ , centered about  $\psi_e = -90^\circ$ . (Page 44, Reference 4). The analysis is simplified by assuming that the range for the OPEP angle is  $\pm 180^\circ$  centered about  $\psi_e = -90^\circ$ .

It follows that  $\cos \gamma_e = \bar{i}_b \cdot \bar{i}_e$ . Define  $C \equiv (\bar{i}_b \times \bar{i}_e) \cdot \bar{k}_b$ .  
 By geometrical considerations the quadrant of  $\gamma_e$  may be determined from  
 the signs of  $\cos \gamma_e$  and  $C$ .

For  $\cos \gamma_e > 0$ ,  $\gamma_e$  is in the 1st or 4th quadrant.

For  $\cos \gamma_e < 0$ ,  $\gamma_e$  is in the 2nd or 3rd quadrant.

For  $C > 0$ ,  $\gamma_e$  is in the 1st or 2nd quadrant.

For  $C < 0$ ,  $\gamma_e$  is in the 3rd or 4th quadrant.

#### 4. Angle Between the Line of Apesides and the Ecliptic Plane $\gamma$

This is the minimum angle between the vector pointing from the center of  
 the Earth to perigee and the ecliptic plane. This angle varies from  $0^\circ$  to  $90^\circ$ .  
 From geometrical considerations it follows that:

$$\sin \gamma = \bar{P} \cdot \bar{k}'$$

where

$$\bar{k}' = -\bar{j} \sin e + \bar{k} \cos e$$

$$\bar{P} = \bar{i}P_x + \bar{j}P_y + \bar{k}P_z$$

$$\bar{P} \cdot \bar{k}' = P_z \cos e - P_y \sin e$$

5. Flight Path Angle  $\gamma$

This is the minimum angle between the satellite's velocity vector  $\dot{\bar{r}}_{VE}$  and the plane normal to  $\bar{r}_{VE}$ . The following formula was used to calculate  $\gamma$  (Page 342, Reference 9):

$$\tan \gamma = \frac{e \sin v}{1 + e \cos v}$$

6. OPEP - Velocity Vector Angle  $\theta$

This is the angle between the vectors  $\bar{i}_e$  and  $\dot{\bar{r}}_{VE}$ .

$$\theta_e = \cos^{-1} \left( \frac{\bar{i}_e \cdot \dot{\bar{r}}_{VE}}{|\dot{\bar{r}}_{VE}|} \right)$$

where  $\bar{i}_e$  is defined on page 12.

7. Angle Between the Projection of the Line of Apesides on the Ecliptic Plane and the Earth-Sun Line  $\xi$

This is the angle between the projection of the  $-\bar{P}$  vector ( $-\bar{P}$  points from the center of the Earth to apogee) on the ecliptic plane and the vector which points from the center of the Earth to the Sun.

$$\xi = \cos^{-1} \left[ \frac{-\bar{k}' \times (\bar{P} \times \bar{k}') \cdot \bar{u}_{SE}}{|\bar{k}' \times (\bar{P} \times \bar{k}')|} \right]$$

8. The Distance From the Center of the Earth to the Satellite,  $r_{VE}$

The following formula was used to calculate  $r_{VE}$  (Page 336, Reference 9);

$$r_{VE} = \frac{a(1-e^2)}{1+e \cos v}$$

D. HEAT INPUTS TO AN ARBITRARILY ORIENTED SURFACE OF EGO

1. Earth Emitted Radiant Heat

The treatment considers the Earth as a black body radiating uniformly at  $T = 250^{\circ} \text{K}$  (Reference 10). The emittance  $\Lambda$  is given by  $\Lambda = \sigma T^4$ , where  $\sigma$  is the Stephan-Boltzman constant and  $T$  is the absolute temperature for a black body. Therefore the average quantity of power radiating into space from the surface of the Earth is  $\Lambda = 0.02215$  watts per square centimeter of the Earth's surface. Some portion of the integrated heat flux radiated from the Earth will be incident upon a surface of the satellite whose unit normal is  $\bar{n}$  (See Figure 3). The heat flux,  $q_E$ , in integral form (See Figure 3) is:

$$q_E = \Lambda \int f_E (\eta, \mu, \rho) dA$$

where

$$f_E (\eta, \mu, \rho) = \frac{\cos \eta \cos \mu}{\pi \rho^2} \text{ if } \cos \eta > 0 \text{ and } \cos \mu > 0.$$

$$f_E (\eta, \mu, \rho) = 0 \text{ if } \cos \eta \leq 0 \text{ or } \cos \mu \leq 0$$

$dA$  = An elemental area of the Earth's surface.

$\bar{n}$  = The unit outward-directed normal of the surface in question.

$\bar{\rho}$  = The vector which points from the Earth's elemental area  $dA$  to the satellite.

$\eta$  = The angle between the outward-directed normal of  $dA$  and the vector  $\bar{\rho}$ . If  $\cos \eta \leq 0$  then the satellite cannot see the area  $dA$ , hence  $f_E \equiv 0$ .

$\mu$  = The angle between the outward-directed normal of the surface,  $\bar{n}$  and the vector  $-\bar{\rho}$  which points from the surface to the area  $dA$ . If  $\cos \mu \leq 0$ , then the surface with normal  $\bar{n}$  cannot see the area  $dA$ , hence  $f_E \equiv 0$ .

Define the Earth emitted radiation factor  $F_E$  by

$$F_E = \frac{q_E}{\Lambda}$$

The values of  $F_E$  have been evaluated in closed form  
(References 10 and 11).

Depending upon the range of  $\lambda$  (where  $\lambda$  is the angle between  $-\bar{r}_{VE}$  and  $\bar{n}$ ) there are three different formulas required for calculating  $F_E$ . They are as follows:

- a. If the surface of the satellite with outward normal  $\bar{n}$  cannot see the Earth (see Figure 4)

$$\lambda \geq \frac{\pi}{2} + \phi_m$$

then  $F_E \equiv 0$

where  $\phi_m = \sin^{-1} \frac{1}{H} =$  the maximum look angle for which the

satellite can see the surface of the Earth.

$H \equiv \frac{r_{VE}}{R_e}$ , where  $r_{VE}$  is the distance from the center of the Earth to the vehicle and  $R_e$  is the equatorial radius of the Earth.

- b. If

$$\frac{\pi}{2} - \phi_m < \lambda < \frac{\pi}{2} + \phi_m$$

$$F_E = \frac{1}{2} - \frac{\sin^{-1} \left[ \frac{(H^2-1)^{\frac{1}{2}}}{H \sin \lambda} \right]}{\pi} +$$

$$\frac{1}{\pi H^2} \cos \lambda \cos^{-1} \left[ -(H^2-1)^{\frac{1}{2}} \cot \lambda \right] -$$

$$\frac{1}{\pi H^2} (H^2-1)^{\frac{1}{2}} \left[ 1-H^2 \cos^2 \lambda \right]^{\frac{1}{2}}$$

For this case, the surface is so oriented that its plane falls within the tangent cone (the cone defining the limits of the visible area of the Earth) so that the surface with unit normal  $\bar{n}$  receives radiation from only a portion of the total area visible from the satellite. (See Figure 5).

c. If

$$0 \leq \lambda \leq \frac{\pi}{2} - \delta_m$$

$$F_E = \frac{\cos \lambda}{H^2},$$

For this case the surface is oriented such that it can see the entire spherical cap which is defined by the tangent cone.

(See. Figure 6).

2. Direct Solar Radiant Heat,  $q_S$  -- The heat flux incident upon the surface of the satellite whose unit normal is  $\bar{n}$ , which arrives directly from the Sun. The fraction of the solar constant  $S$  which is incident upon this surface of the satellite is

$$F_S = \frac{q_S}{S} \cong \frac{\bar{n} \cdot \bar{r}_{SV}}{|\bar{r}_{SV}|}$$

3. Reflected Solar Radiant Heat  $q_o$  -- The heat flux incident upon the surface of the satellite whose unit normal is  $\bar{n}$ , which originates at the Sun and reflects from the Earth to the satellite. In integral form (see Figure 3).

$$q_o = S_o \int f_o (\eta, \mu, \beta, \rho) dA$$

where

$$f_o (\eta, \mu, \beta, \rho) = \frac{\cos \eta \cos \mu \cos \beta}{r \rho^2}$$

if

$$\cos \eta > 0, \cos \mu > 0 \text{ and } \cos \beta > 0$$

and

$$f_o (\eta, \mu, \beta, \rho) = 0$$

$$\text{if } \cos \eta \leq 0 \text{ or } \cos \mu \leq 0 \text{ or } \cos \beta \leq 0$$

$c$  = the albedo = the fraction of the solar constant which is reflected away from the Earth. ( $c = .34$  for this study, Reference 12).

$\beta$  = The angle between the vector  $\bar{u}_{SE}$  and the outward-directed normal of the Earth's elemental surface area  $dA$  (See Figure 3).

If  $\cos \beta \leq 0$ , then that portion of the Earth's surface  $dA$  is not lighted by the Sun,  $f_o = 0$ .

A closed form solution could not be found for this integral. Its value was approximated by assuming an average value for  $\cos \beta$ . It was assumed that  $\cos \beta$  (average) =  $\cos \theta_S$  (See Figure 3) where

$\theta_S$  = The angle between the unit vector  $\bar{u}_{SE}$  and the vector  $\bar{r}_{VE}$ .

This reduces the integral to the same form as  $q_E$ . (see page 22).

Hence, the approximate expression for  $q_c$  becomes

$$q_c \approx c S \cos \theta_S F_E$$

where the closed form solution for  $F_E$  is presented on page 23.

Define

$$F_c = \frac{q_c}{cS} \approx F_E \cos \theta_S$$

except when

$$\cos \theta_S \leq 0$$

then

$$F_c = 0$$

because

$F_c$  cannot be a negative quantity.

Figure 7 presents a comparison between  $q_c$  (approximate) and  $q_c$  (actual) as a function of altitude with  $\lambda$  and  $\theta_S$  as parameters. The values of  $q_c$  (approximate) were calculated using the simplified formula presented on page 27. The values of  $q_c$  (actual) were determined by numerical evaluation of the integral on page 26 of this report for  $\xi_c = 180^\circ$ . For this value of  $\xi_c$  the difference between  $q_c$  (approximate) and  $q_c$  (actual) is maximized; the difference was calculated to be less than  $2 \text{ mw/cm}^2$  as shown on Figure 7. The angle  $\xi_c$  is the angle between the plane formed by the vectors  $\bar{r}_{VE}$  and  $\bar{r}_{SE}$ ; and the plane formed by the vectors  $\bar{r}_{VE}$  and  $\bar{n}$  (See Figure 8). The value of  $q_c$  (actual) is a function of  $r_{VE}$ ,  $\lambda$ ,  $\theta_S$  and  $\xi_c$ ; whereas  $q_c$  (approximate) is a function of  $r_{VE}$ ,  $\lambda$ ,  $\theta_S$ , but not a function of  $\xi_c$ . Figure 7 shows that the maximum difference between the two methods occurs at the lower altitudes. The difference becomes insignificantly small at altitudes greater than 20,000 N.M. The formula for  $q_c$  (approximate) breaks down for  $\theta_S = 90^\circ$ , but  $q_c$  (actual) becomes insignificantly small and can be approximated to zero. The  $q_c$  approximation is adequate when compared to the uncertainties in the albedo, e.g., the albedo varies between 0.3 and 0.6 depending on the latitude and season (Reference 13). The maximum difference between  $q_c$  (approximate) and  $q_c$  (actual) is only 1.3% of the solar constant.

## V. COMPUTER PROGRAMS

### A. The Launch Window Program.

The basic Launch Window Program was developed by P. Musen with the assistance of A. Smith (both of the Theoretical Division; Goddard Space Flight Center). R. Devaney, also of Goddard, made the changes for

its adaptation to the OGO problems. A description of the basic Launch Window Program, including a bibliography, is presented in Reference 1.

The input quantities are the orbit elements  $a_0$ ,  $e_0$ ,  $i_0$ ,  $\Omega_0$  and  $\omega_0$  at the initial time  $\tau_0$ . The program calculates  $a$ ,  $e$ ,  $i$ ,  $\Omega$ , and  $\omega$  for time  $\tau$ , taking into account the influence of the gravitational forces due to the Moon, the Sun and the Earth, including the 2nd, 3rd and 4th zonal harmonics. The time per orbit that the satellite spends in the Earth's shadow is also computed by the program. The program does not calculate the position of the spacecraft in its orbit.

The orientation of the orbit in space is defined by the unit vectors  $\bar{P}$ ,  $\bar{Q}$  and  $\bar{R}$ . These are given in terms of  $i$ ,  $\Omega$ , and  $\omega$  in Reference 8.

#### B. The Interplanetary Trajectory Program (IPP)

This program (Reference 14) was used to check the behavior of the orbital elements as a function of time. (Reference 1). The IPP can be used to calculate the position and velocity of the satellite relative to the Earth as a function of time when given an initial set of injection conditions. The launch window program does not have this capability. The launch window program calculates the spacecraft angular data presented in this report, to a sufficiently high degree of accuracy that it may be used with confidence in most cases. All of the angle and heat input calculations presented in this report will be programmed into the IPP (with its accurate position calculation) and will be available for post flight analysis of the EGO (S-49) satellite.

## VI. RESULTS AND DISCUSSION

### A. Orbital Parameters and Spacecraft Angles

The results of orbit parameter studies for EGO are shown graphically on Figures 9 through 16. These studies are based on a launch date of November 6, 1963 at 16.0, 20.0 and 24.0 hours U.T. The elements of the initial orbits are:

$$\begin{aligned} a &= 9.731167 \quad \text{Earth radii} \\ e &= .8929018 \\ i &= 30^{\circ}.807 \\ \omega &= -45^{\circ}.596 \\ \Omega_1 &= 75^{\circ}.27 \quad \text{for 16.0 hours U.T.} \\ \Omega_2 &= 135^{\circ}.43 \quad \text{for 20.0 hours U.T.} \\ \Omega_3 &= 195^{\circ}.59 \quad \text{for 24.0 hours U.T.} \end{aligned}$$

These elements are consistent with the initial conditions of Part III on page 10.

Due to the large semi-major axis ( $a = 9.73117$  Earth Radii), the period for EGO is 42.75 hours. The orbit has great variations in the speed of the spacecraft throughout its orbit, especially near perigee, as can be seen in the rapid variations in true anomaly, solar array angle, OPEP angle, flight path angle, OPEP-velocity vector angle, and in the distance from the center of the Earth to the satellite; shown on Figures 9, 10, 11, 13, 14 and 16, respectively.

1. True anomaly,  $v$

Figure 9 shows the true anomaly variation with time for one orbital period. The computation was done with two-body equations and the orbital elements at the time of injection were used for this computation. This is a typical curve and its shape will change slightly throughout the year as the orbit changes due to perturbations.

2. Solar array angle,  $\gamma_p$

Figure 10 shows the history of the solar array angle for one orbital period. The angle history varies as a function of injection time into orbit due to the motion of the Earth and Sun. Figure 10 shows the angle histories for three different injection times.

3. OPEP angle,  $\psi_e$

The OPEP angle variation with time is shown on Figure 11 and like the solar array angle its history is a function of injection time (a curve is shown for three injection times).

4. Angle between the line of apsides and the ecliptic plane,  $\psi$

Figure 12 shows the variation of angle between the line of apsides and the ecliptic plane for one year for three different injection times of a given launch day. The absolute value of the expression for  $\sin \psi$  is chosen so that the angle shown on Figure 12 will always lie between  $0^\circ$  to  $90^\circ$ . Hence, in this study the value of the angle  $\psi$  is shown without regard to quadrant.

5. Flight path angle,  $\gamma$

The flight path angle varies periodically with each complete orbit and changes only as the shape of the orbit changes.

Figure 13 shows the flight path angle for one orbital period measured from perigee. The Launch Window Program has the capability of generating this angle at any time. The history of the angle for any orbit during the first year will not differ greatly from Fig. 13.

6. OPEP - Velocity Vector Angle,  $\theta_e$

The variation of the angle between the  $x_e$  axis of orbit plane experiment package (OPEP) and the satellite's velocity vector will be periodic with each orbital period. Figure 14 shows the angle as a function of time. This is a typical curve and will change only slightly throughout the year. The shape of the curve is independent of launch time. Since the absolute value of the expression for  $\theta_e$  is used, the angle is shown on the figure without regard to the quadrant (See Part IV, Section C-6).

7. Angle Between the Projection of the Line of Apsides on the Ecliptic Plane and the Earth-Sun Line,  $\zeta$

Since the motion of the perigee point ( $\dot{\omega}$ ) and the precession of the line of nodes ( $\dot{\Omega}$ ) always maintain the same sign the projection of the line of apsides on the ecliptic plane will continually revolve. Consequently, the angle between the projection of the line of apsides on the ecliptic plane and the Earth-Sun line will continually

vary from zero to  $2\pi$  radians. It facilitates computation to show this angle varying only through  $180^\circ$ , i.e., the smaller of the angles between the projection of the line of apsides on the ecliptic plane and the Earth-Sun line. (See Figure 15). The curves on Figure 15 show the periodic angle variation for three different injection times of a given launch day. The different curves as a function of injection time are due to the change in position of the injection point with respect to the inertial frame because of the Earth's rotation.

8. The distance from the center of the Earth to the satellite,  $r_{VE}$   
Since the orbit for the EGO satellite is non-circular the distance between the spacecraft and the center of the Earth will vary periodically with each orbit. (See Figure 16). The change in the periodicity and amplitude will vary only slightly during the first year of life of the satellite.

#### B. Heat Inputs to EGO

Figures 17 through 25 present the heat inputs incident upon the different faces (Figure 1) of the satellite as a function of time from perigee for the first orbital period (42.75 hours). The data in these figures are based on a time of injection into orbit of November 6, 1963, at 24.0 hours U.T. These curves are intended to demonstrate the capability to calculate heat inputs rather than to provide design data. The Earth

emitted and solar reflected heat inputs are negligibly small when the satellite is beyond an altitude of 20,000 nautical miles or correspondingly 2.63 hours flight time from perigee.

1. Main box

a. Earth emitted

Figure 17 presents the Earth emitted heat inputs ( $q_E$ ) to the main box as a function of time from perigee. The  $+z_b$  face has the largest Earth emitted heat input since it always faces the Earth. Conversely, the  $-z_b$  face has a zero Earth emitted heat input. The  $+x_b$ ,  $-x_b$ ,  $+y_b$ , and  $-y_b$  faces all have equal Earth emitted heat inputs due to geometrical symmetry with respect to the Earth. The curve shown is independent of launch time.

b. Direct solar

Figure 18 presents the direct solar heat inputs ( $q_S$ ) to the main box as a function of time from perigee. This is a typical curve. The solar heat inputs to the  $+x_b$ ,  $-x_b$  and  $+y_b$  face are always zero (see page 12 of this report).

The maximum solar input to any other face is 137.4 milliwatts/cm<sup>2</sup> which would occur when the Sun's rays are normal to a particular surface.

c. Reflected solar

Figure 19 presents the reflected solar heat inputs ( $q_r$ ) to the main box as a function of time from perigee. The  $+z_b$  face has the

largest reflected solar heat input since it faces the Earth. The  
 -  $z_b$  face has zero reflected solar heat input. The +  $x_b$ , -  $x_b$ , +  $y_b$ ,  
 -  $y_b$  faces all have equal reflected solar inputs since it is assumed  
 that  $q_a$  (approximate) is independent of  $\phi_c$ . For this launch date  
 (November 6, 1963, 24.0 hours U.T.) the angle between  $\bar{r}_{SV}$  and  $\bar{r}_{VE}$  was  
 $\theta_S = 63.3^\circ$  at perigee and the solar reflected heats are  $q_a = 6.78$   
 milliwatts/cm<sup>2</sup> on the +  $x_b$ , -  $x_b$ , +  $y_b$  and -  $y_b$  faces; and 19.32  
 milliwatts/cm<sup>2</sup> on the +  $z_b$  face.

## 2. Solar Array

### a. Earth emitted

Figure 20 presents the Earth emitted heat inputs ( $q_E$ ) to the  
 solar array as a function of time from perigee. The +  $x_p$  and -  $x_p$  faces  
 of the solar array have the same Earth emitted heat inputs as the  
 +  $x_b$  and -  $x_b$  face of the main box (See Figure 1). The Earth emitted  
 heat inputs ( $q_E$ ) to the +  $y_p$ , -  $y_p$ , +  $z_p$  and -  $z_p$  faces are also  
 included on this figure.

### b. Direct solar

Figure 21 presents the direct solar heat inputs ( $q_S$ ) to the  
 solar array as a function of time from perigee. Since the +  $y_p$  face  
 of the solar array contains the solar cells and looks directly at the  
 Sun (See page 11 of this report) the heat into this face is the full  
 value of the solar constant  $S = 137.4$  milliwatts/cm<sup>2</sup>. The direct  
 solar heat inputs to the other faces of the array -  $y_p$ , +  $x_p$ , -  $x_p$ , +  $z_p$   
 -  $z_p$  are all zero.

### c. Reflected solar

Figure 22 presents the reflected solar heat inputs ( $q_o$ ) to the solar array as a function of time from perigee. The  $+x_p$  and  $-x_p$  faces of the solar array have the same reflected solar heat inputs as the  $+x_b$  and  $-x_b$  face of the main box. The reflected solar heat inputs to the  $+y_p$ ,  $-y_p$ ,  $+z_p$  and  $-z_p$  faces are also included in this figure.

## 3. Orbit Plane Experiment Package (OPEP)

### a. Earth emitted

Figure 23 presents the Earth emitted heat inputs ( $q_E$ ) to the OPEP as a function of time from perigee. The  $+z_e$  face has the same Earth emitted heat inputs as the  $+z_b$  face of the main box since both faces are oriented the same way. The  $-z_e$  face has a zero Earth emitted heat input since it never faces the Earth. The  $+x_e$ ,  $-x_e$ ,  $+y_e$ ,  $-y_e$  faces all have equal Earth emitted heat inputs due to geometrical symmetry with respect to the Earth.

### b. Direct solar

Figure 24 presents the direct solar heat inputs ( $q_S$ ) to the OPEP as a function of time from perigee. The solar heat inputs to the  $+z_e$  and  $-z_e$  faces are the same as to the  $+z_b$  and  $-z_b$  faces of the main box, respectively. The solar inputs to the  $+y_e$  and  $-y_e$  faces are nearly constant over one orbital period since these faces are parallel to the orbit plane and since the angle between the Earth-Sun

line and the plane of the orbit is nearly constant over one orbital period. The direct solar heat inputs to the  $+x_e$  and  $-x_e$  faces are also included on the figure.

c. Reflected solar

Figure 25 presents the reflected solar heat inputs ( $q_r$ ) to the OPEP as a function of time from perigee. The  $+z_e$  face has the same reflected solar heat input as the  $+z_b$  face of the main box since both faces are oriented the same way. The  $-z_e$  face has zero solar reflected heat input, since it never faces the Earth. The  $+x_e$ ,  $-x_e$ ,  $+y_e$ ,  $-y_e$  all have equal solar reflected heat inputs due to geometric symmetry with respect to the Earth.

ACKNOWLEDGEMENT

The authors gratefully acknowledge the valuable help of Dr. H. Wolf for formulation of analysis, of R. Devaney for programming and of J. Chiville for assistance in the preparation of graphic presentations.

## VII. CONCLUSIONS

The methods of analyzing the orbital parameters, the spacecraft angles and the spacecraft heat inputs presented in this document were developed primarily to do a pre-launch study of the Eccentric Orbiting Geophysical Observatory, S-49 (EGO), but the methods are general and may be applied to any near Earth satellite. These methods especially have application for studies on future Orbiting Geophysical Observatories (e.g., POGO).

The program developed as a result of this study is a modified Halphen method program. The basic program was conceived by P. A. Musen and subsequently modified for use as a launch window program for EGO. Flexibility in the choice of control laws makes the program appealing for general use. A secondary but important advantage of the program is that a year study may be computed in about three minutes on the IBM 7094.

The closed form solution of the solar reflected heat input developed in this document, while being an approximation, was found to be quite accurate. The maximum error resulting from the use of the closed form solution is only 1.3% of the solar constant, and it is not restricted to the problem treated.

The program has been named the "Launch Window Program". It has been designed for use on IBM 7094 computer but can be easily adapted for other computing systems.

## VIII. REFERENCES

1. Montgomery, H. E., EGO Launch Window Study, NASA Report X643-62-225, Goddard Space Flight Center, Greenbelt, Maryland.
2. Hemenover, A. P., Nominal Trajectory and Impact Data of EOGO Mission, Lockheed Missiles and Space Company Report No. A-306775/91-21, dated November 9, 1962, Sunnyvale, California.
3. Specification for the Orbiting Geophysical Observatory, S-49/50 Revision 1, dated August 1962, Goddard Space Flight Center, Greenbelt, Maryland.
4. Otten, D. D., OGO Attitude Control Subsystem Description, Logic, and Specifications, Report Number 2313-0004-RV-000, 4 December 1961, Space Technology Laboratories, Inc., Redondo Beach, California.
5. Moulton, F. R., Celestial Mechanics, Macmillan, New York, 1914.
6. Clarke, Victor C., Constants and Related Data Used in Trajectory Calculations at the Jet Propulsion Laboratory, Technical Report Number 32-273, May 1, 1962, Jet Propulsion Laboratory, California Institute of Technology, Pasadena, California.
7. The American Ephemeris and Nautical Almanac, 1960, United States Government Printing Office, Washington, D. C.
8. Baker, Robert M. L. and Makemson, Maud W., An Introduction to Astrodynamics, Academic Press, New York.
9. Kraft, Ehricke A., Space Flight, Volume 1, D. Van Nostrand Company, Inc.
10. Cunningham, F. G., Power Input to a Small Flat Plate From a Diffusely Radiating Sphere, With Application to Earth Satellites, NASA TN D-710, August, 1961, Goddard Space Flight Center, Greenbelt, Maryland.

11. Stevenson, J. A. and Grafton, J. C., Radiation Heat Transfer Analysis for Space Vehicles, ASD Technical Report 61-119, Space and Information Systems Division, North American Aviation, Inc.
12. Allen, C. W., Astrophysical Quantities, University of London, The Athlone Press, 1955, Published in the U.S.A. by Essential Books, Fairlawn, New Jersey.
13. Johnson, John C., Physical Meteorology, John Wiley and Sons, Inc., New York, 1954.
14. Pines, S., and Wolf, H., Interplanetary Trajectory by the Encke Method Programmed for the IBM 7090, Report No. RAC-656-451, 12 December, 1960, Research and Development Division Republic Aviation Corporation, Farmingdale, Long Island, New York.

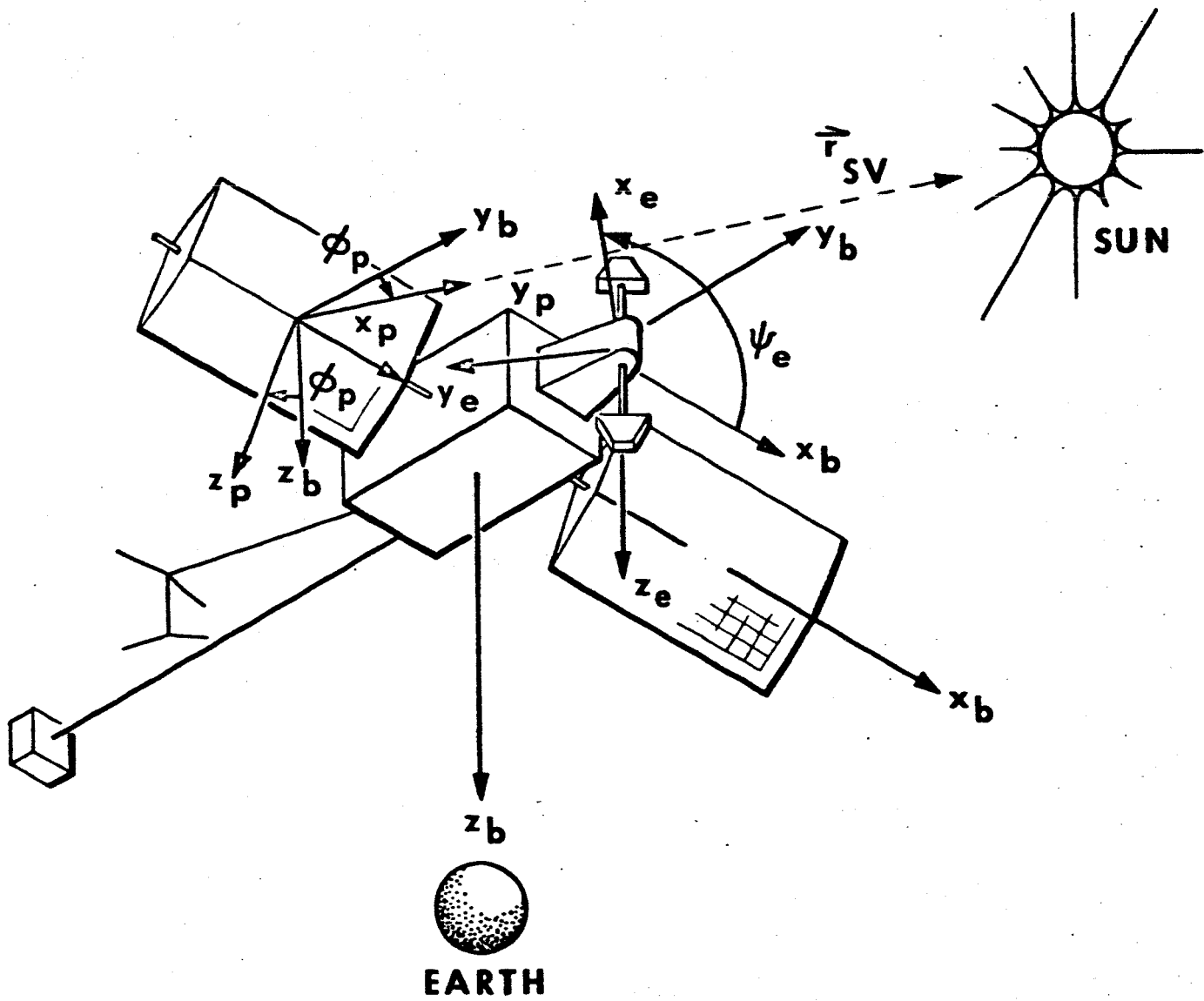


Fig. 1 Body Coordinate System

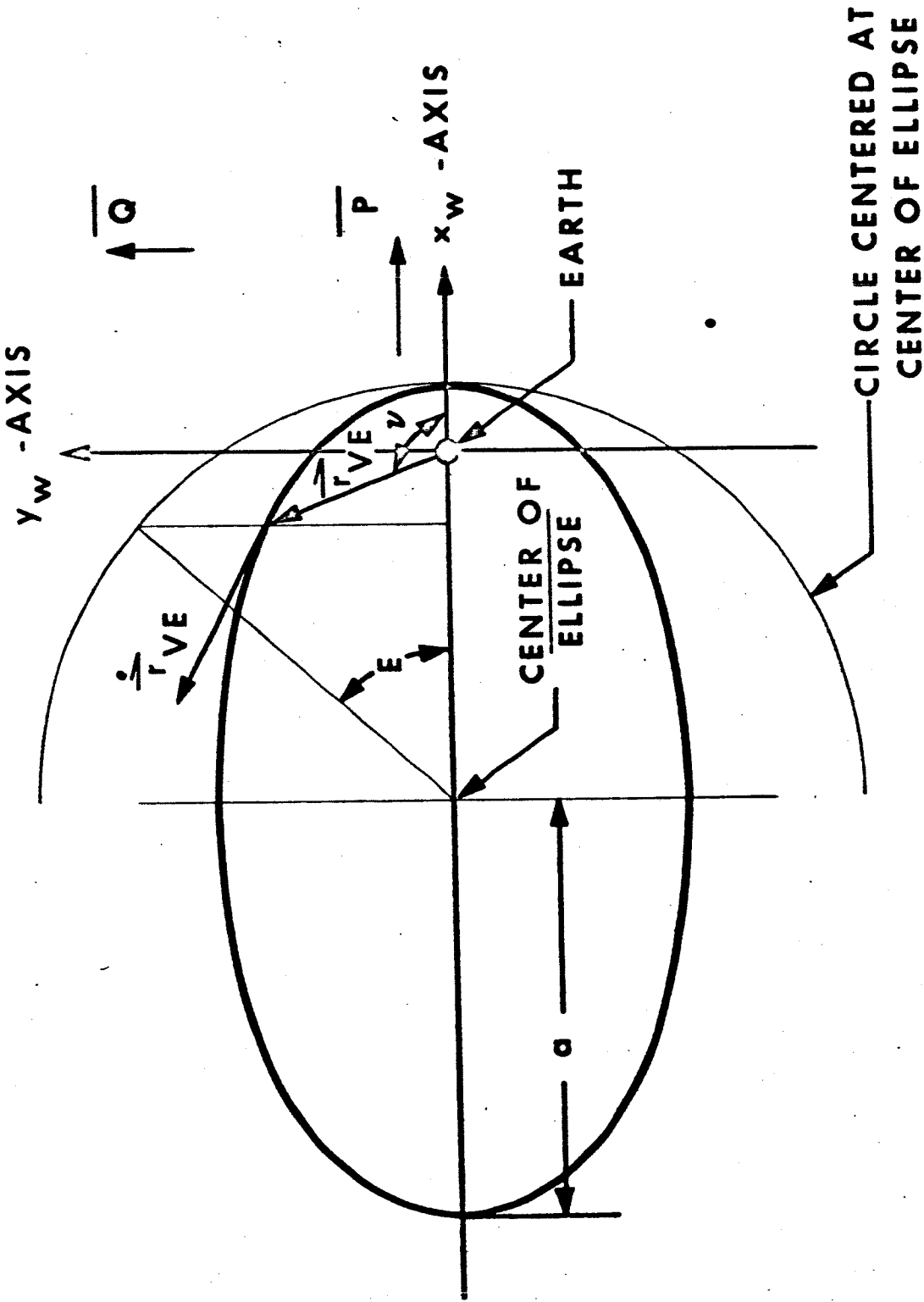


Fig. 2 Geometry of the Elliptic Two Body Orbit

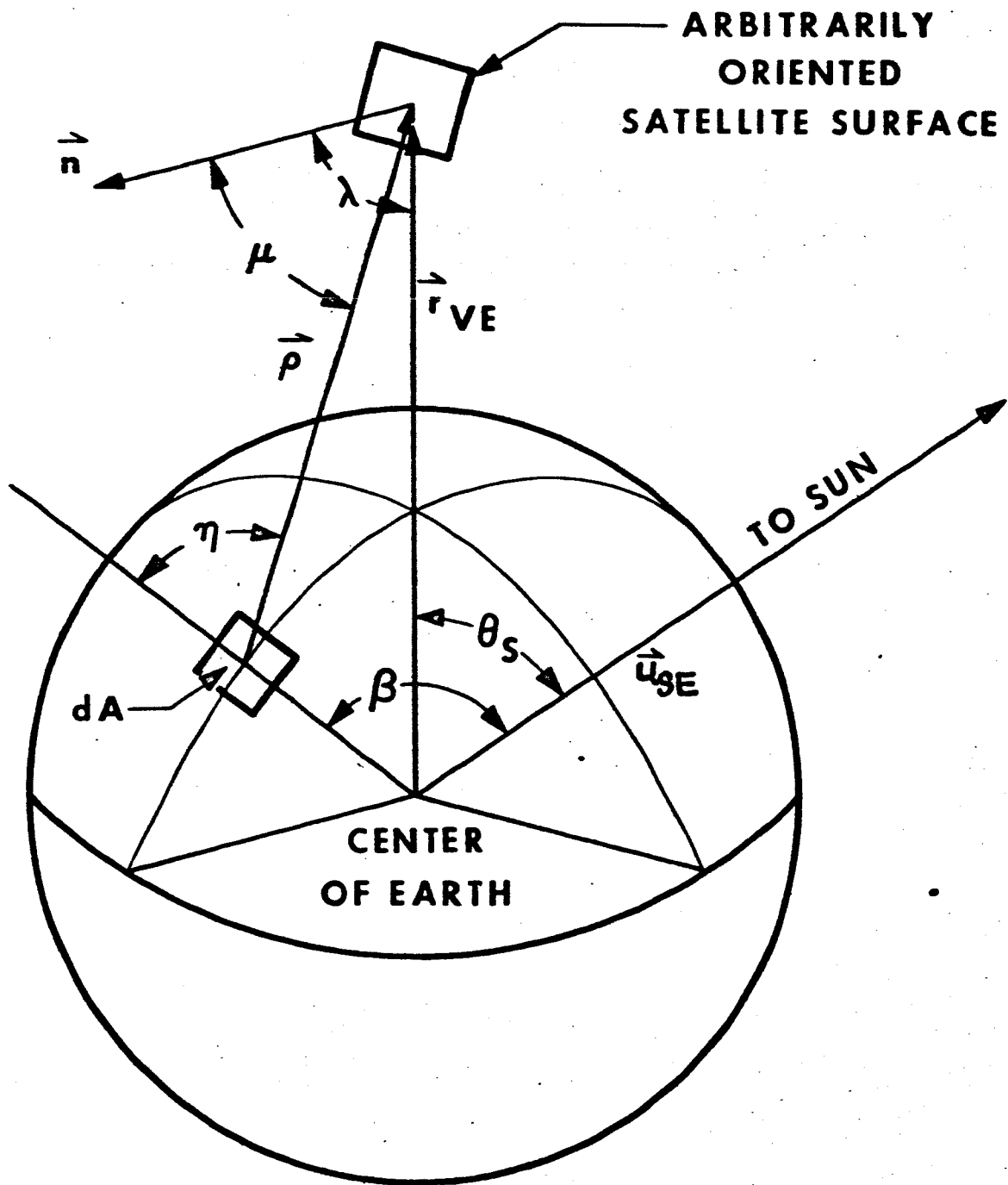
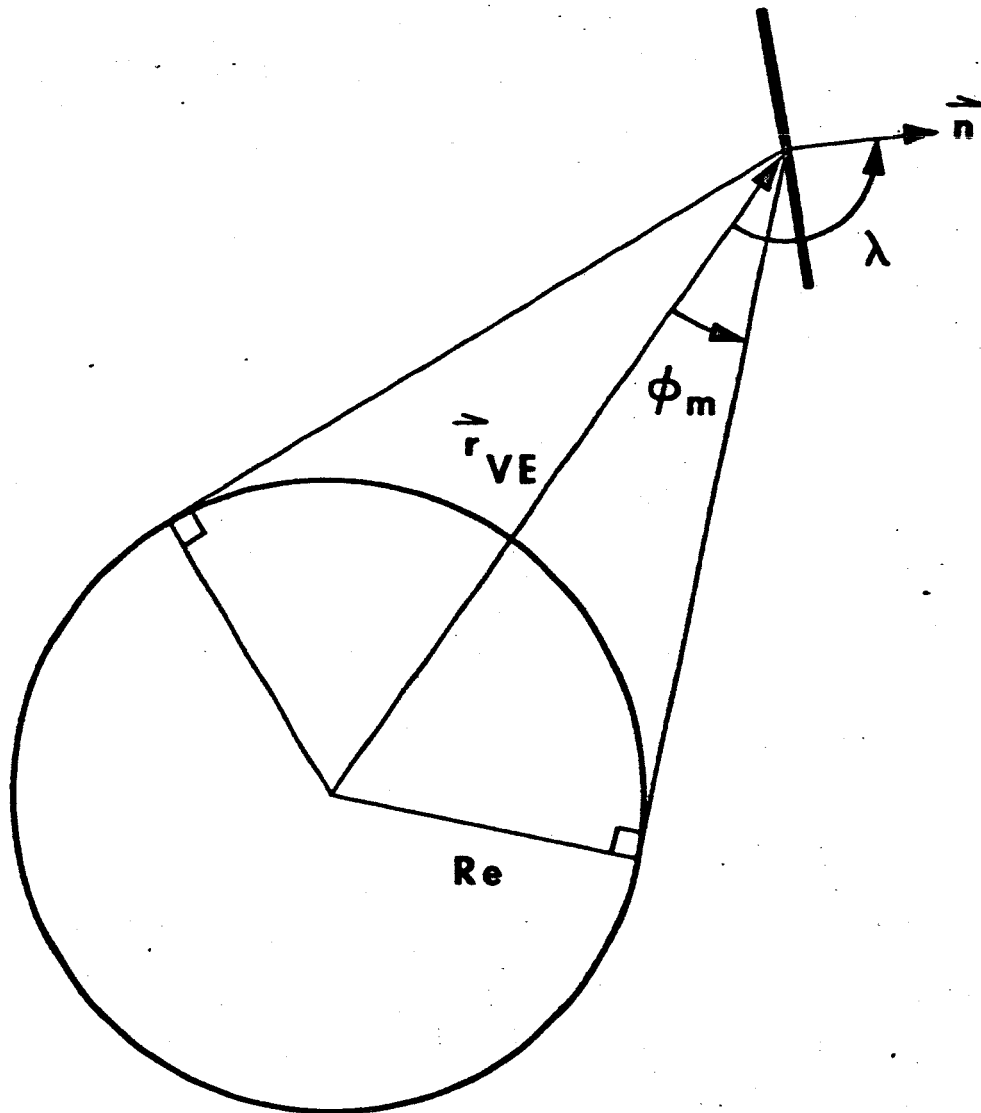


Fig. 3 Geometry for Heat Inputs

**CASE 1. SATELLITE SURFACE WITH UNIT NORMAL  $\vec{n}$   
CANNOT SEE THE EARTH.**



**Fig. 4 Geometry for Earth Emitted Heat Inputs**

CASE 2. SATELLITE WITH UNIT NORMAL  $\vec{n}$  CAN SEE A PORTION OF THE EARTH'S SURFACE WITHIN THE TANGENT CONE.

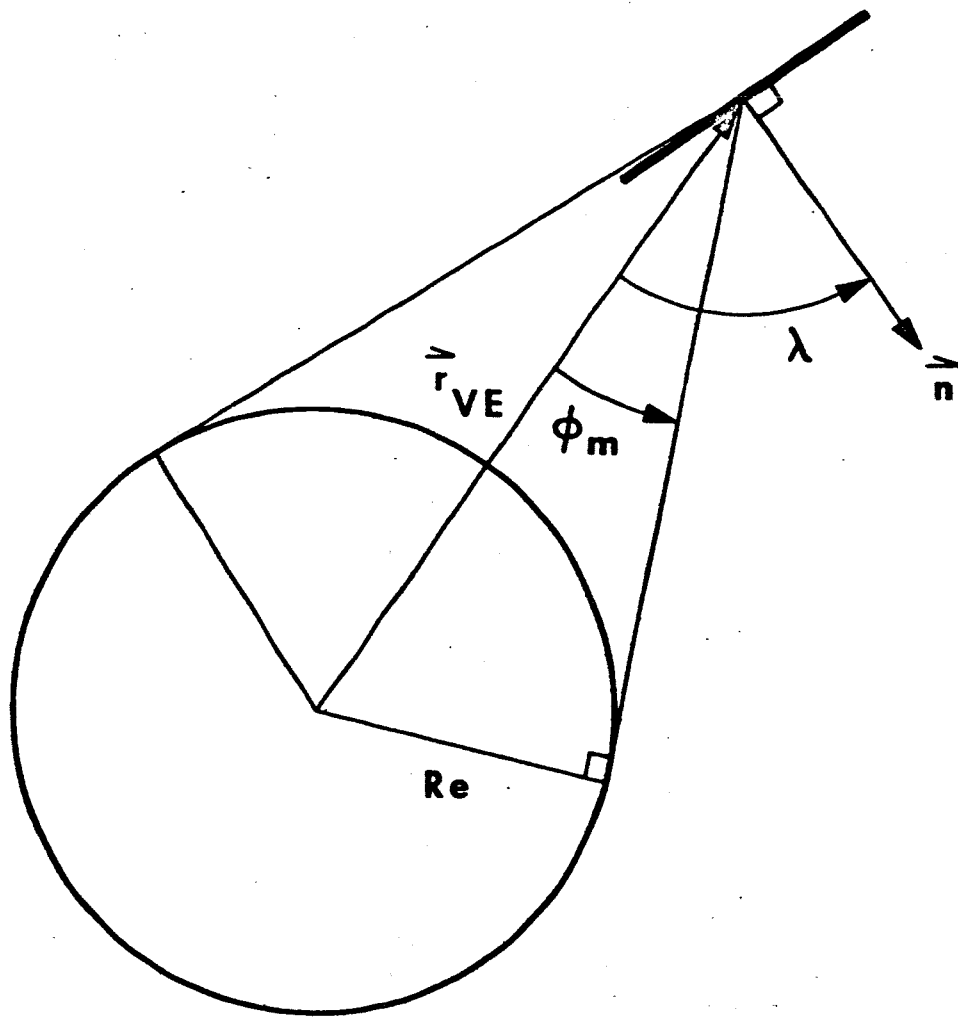
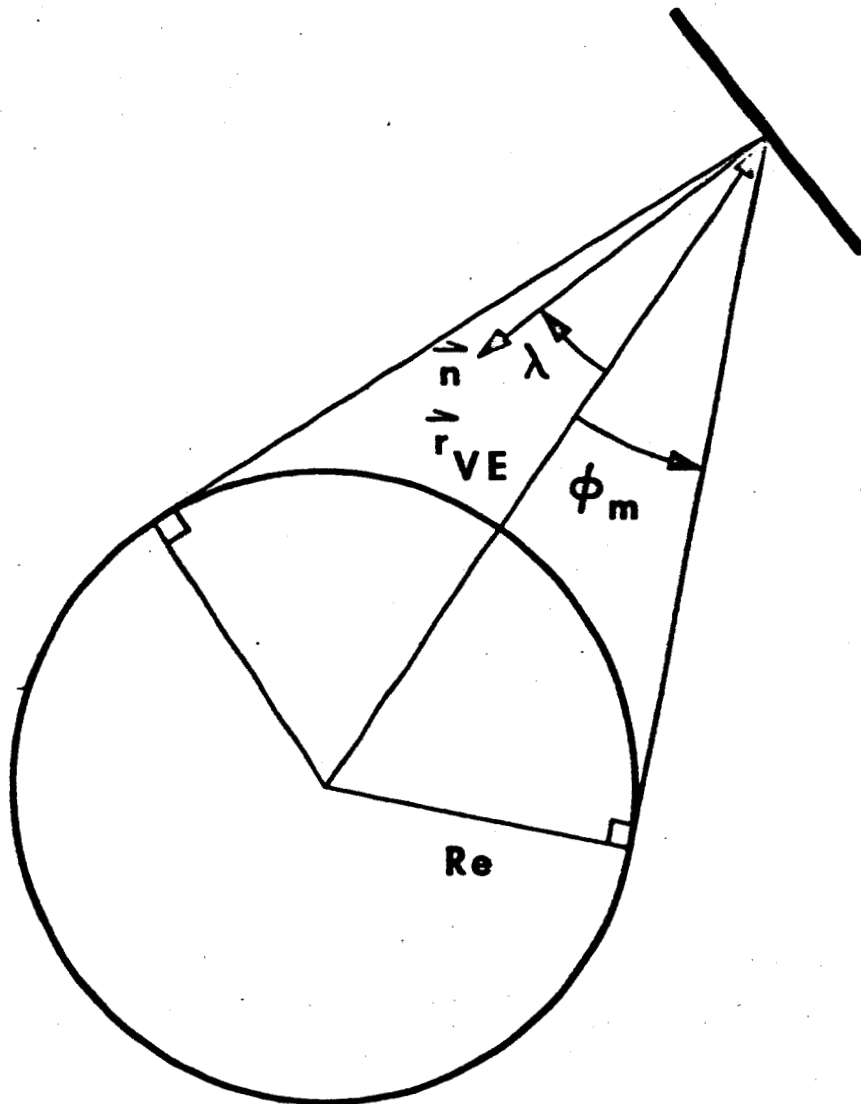


Fig. 5 Geometry for Earth Emitted Heat Inputs

**CASE 3. SATELLITE SURFACE WITH UNIT NORMAL  $\vec{n}$  CAN SEE THE ENTIRE SURFACE WITHIN THE TANGENT CONE.**



**Fig. 6 Geometry for Earth Emitted Heat Inputs**

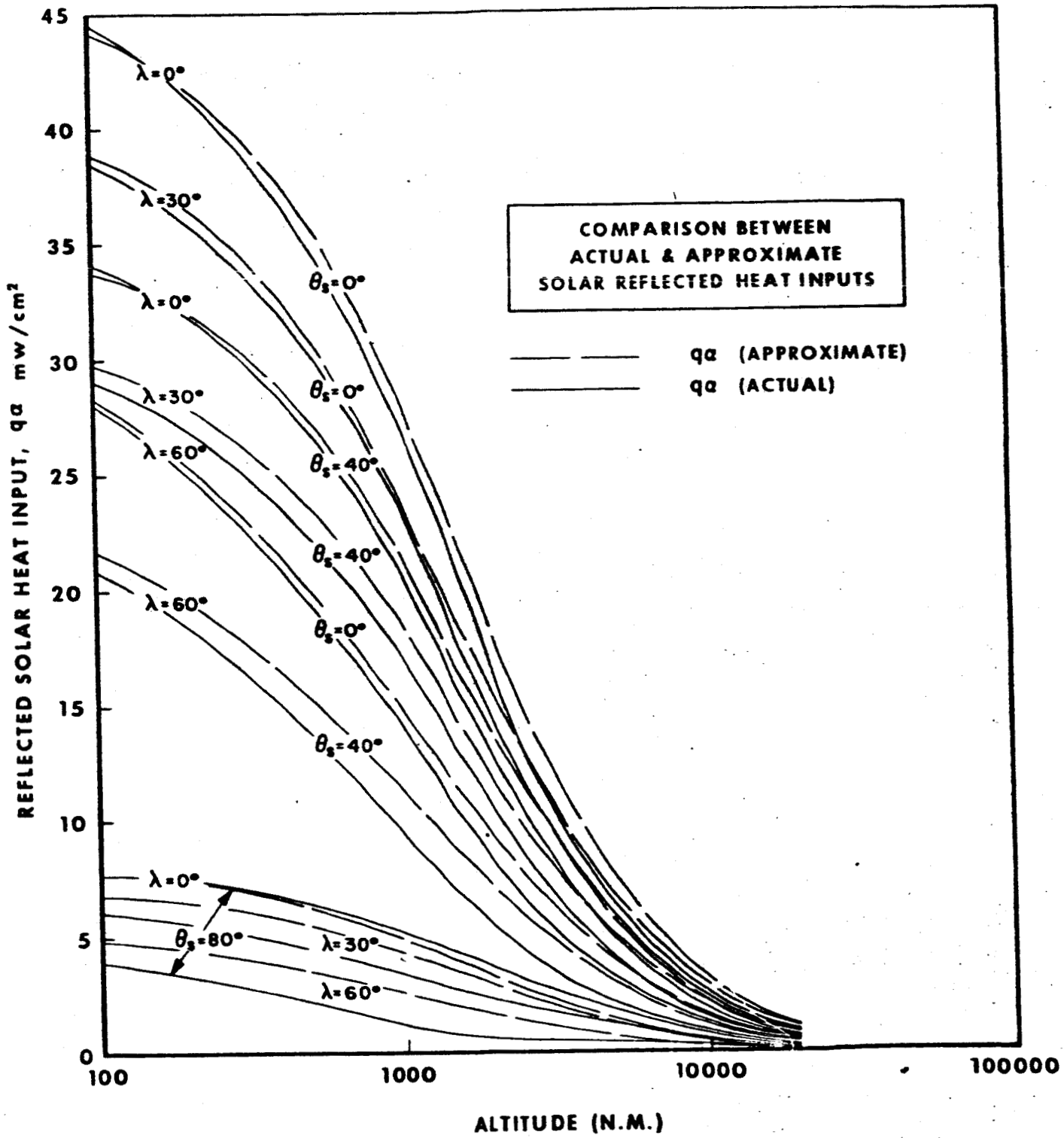
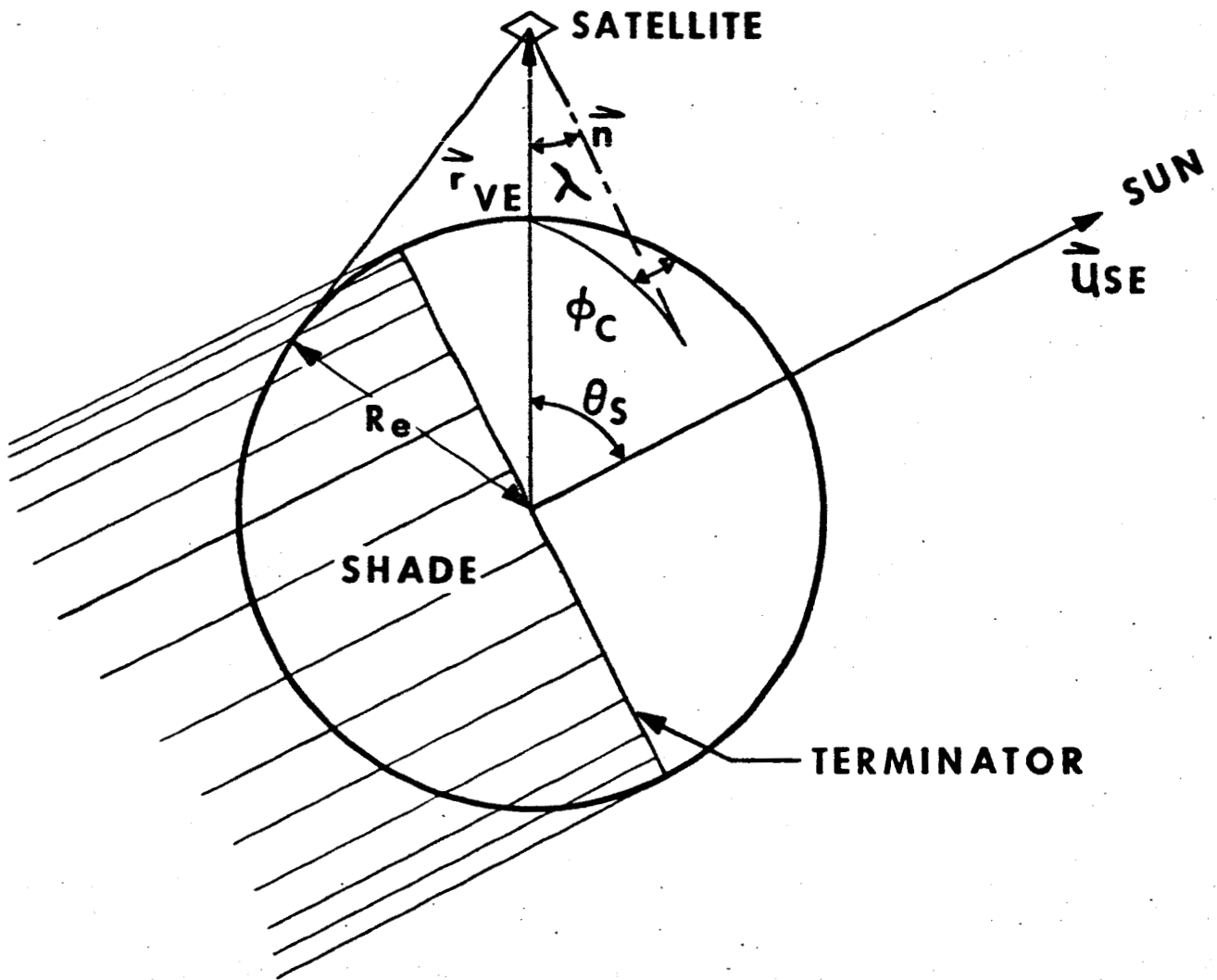
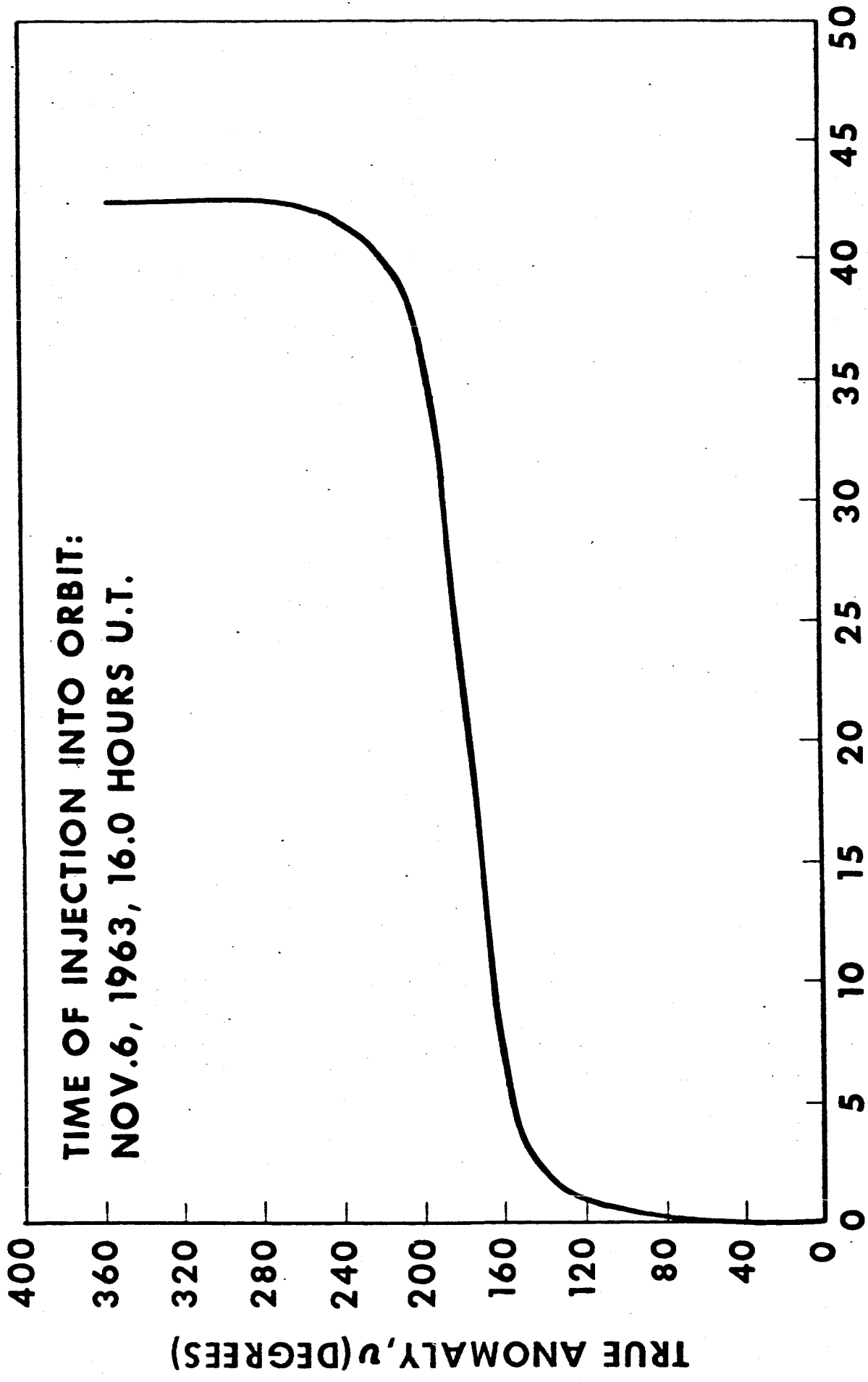


FIGURE 7.



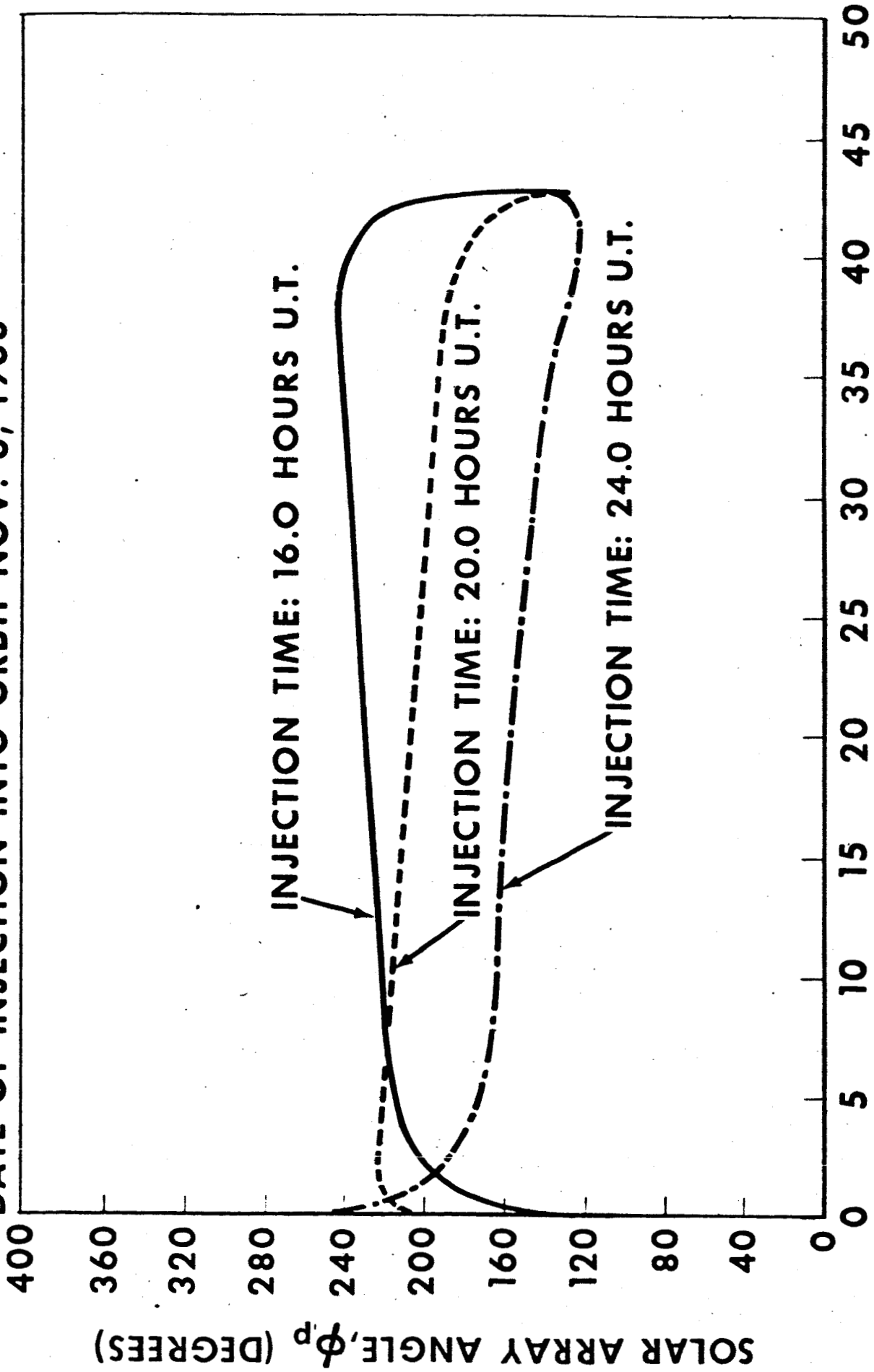
**Fig. 8 Geometry for Reflected Solar Heat Inputs**



**TIME FROM PERIGEE (HOURS)**

**Figure 9. True anomaly**

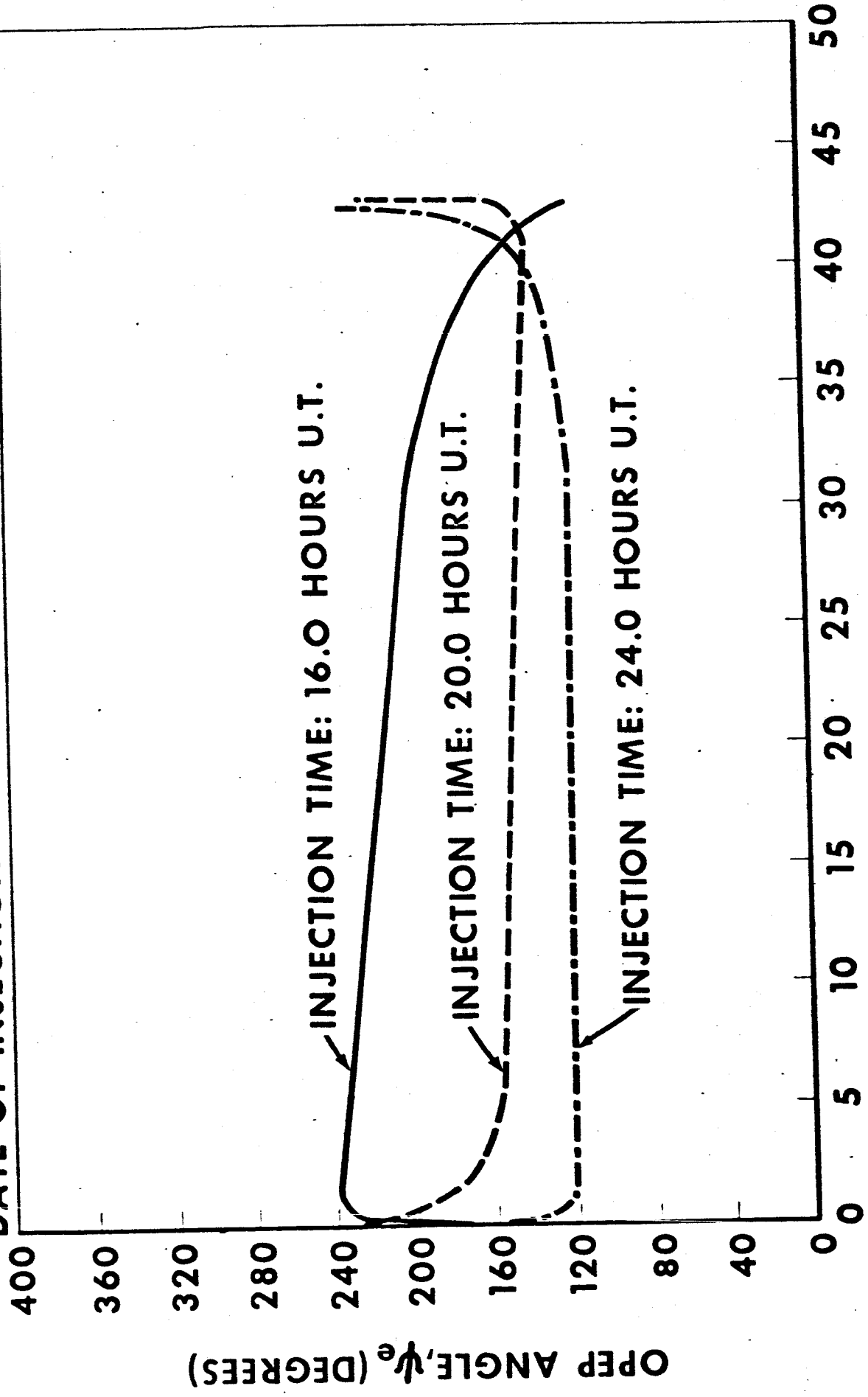
DATE OF INJECTION INTO ORBIT NOV. 6, 1963



TIME FROM PERIGEE (HOURS)

Figure 10. Solar array angle

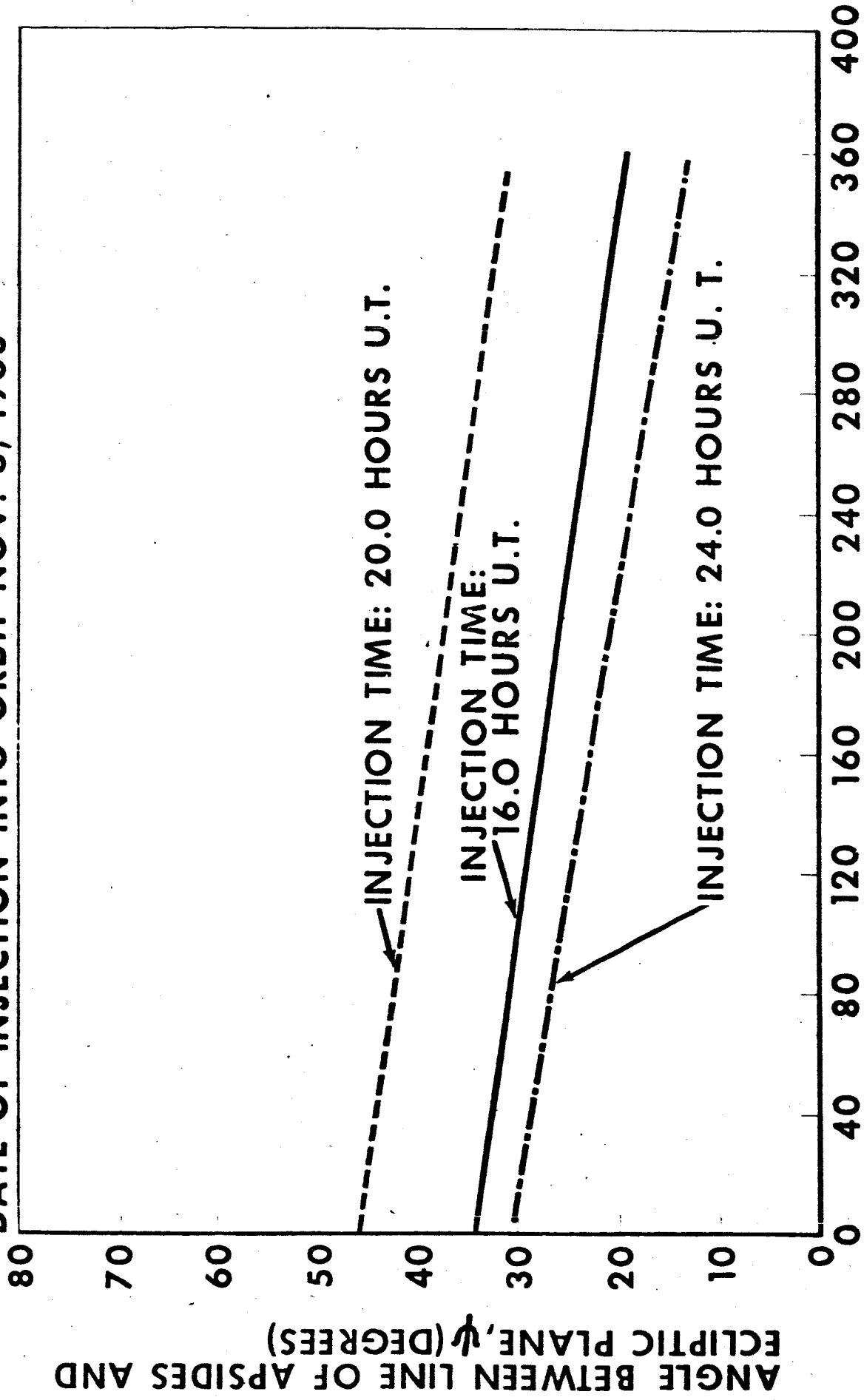
DATE OF INJECTION INTO ORBIT NOV. 6, 1963



TIME FROM PERIGEE (HOURS)

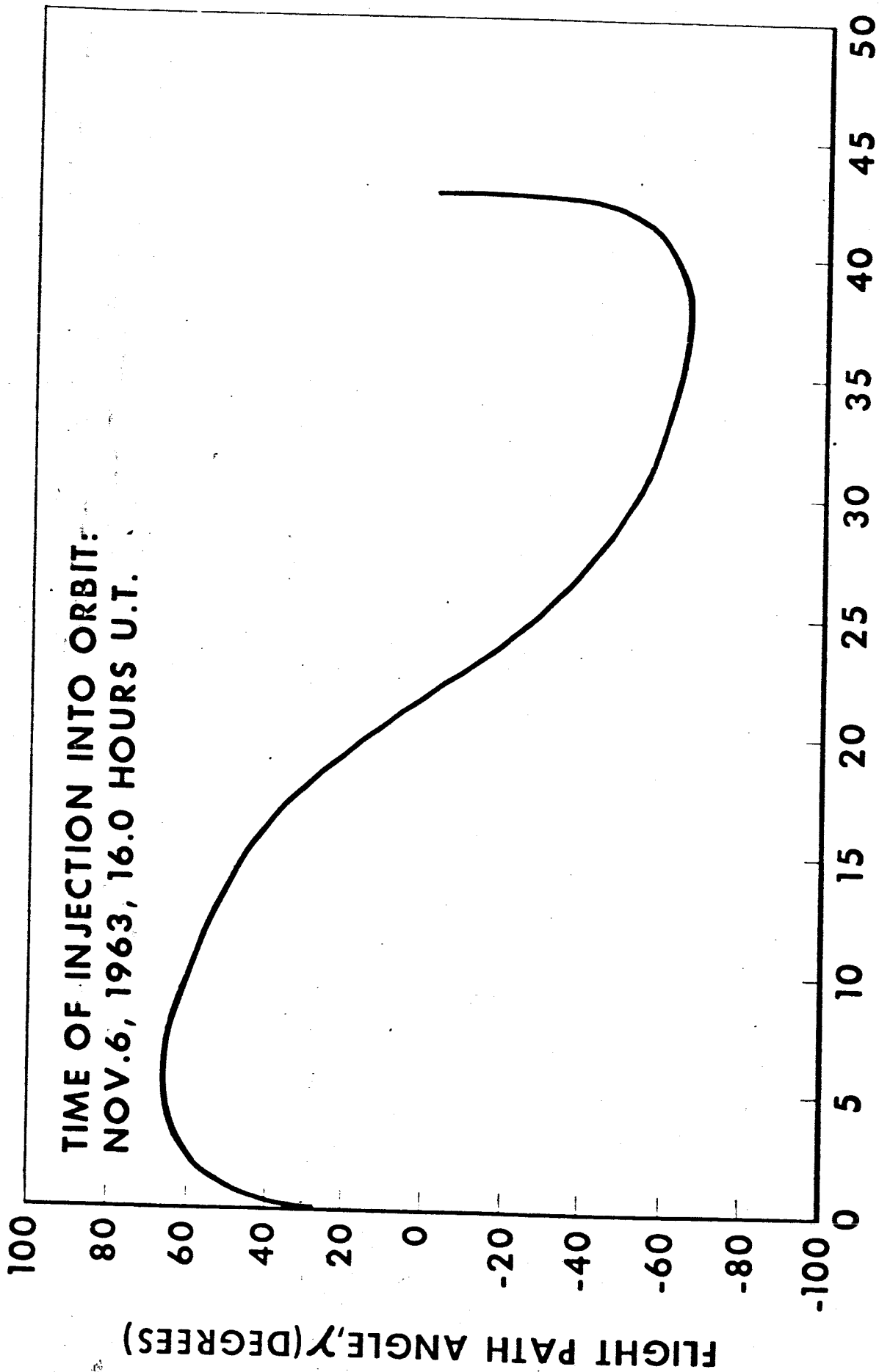
Figure 11. Opep-angle

DATE OF INJECTION INTO ORBIT NOV. 6, 1963



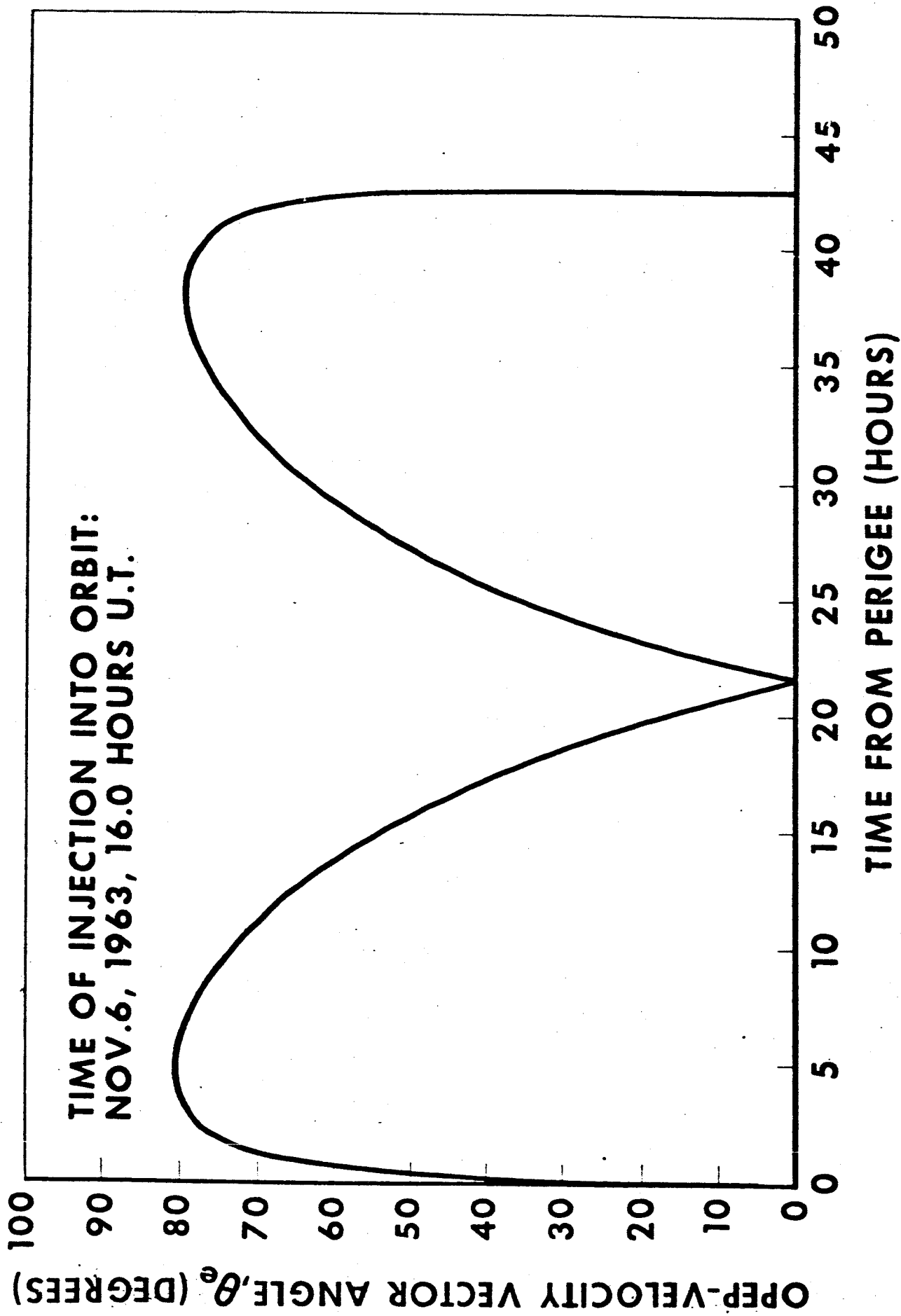
DAYS FROM LAUNCH

Figure 12. Apsides-ecliptic angle



**TIME FROM PERIGEE (HOURS)**

**Figure 13. Flight path angle.**



**Figure 14. Opep-velocity vector angle.**

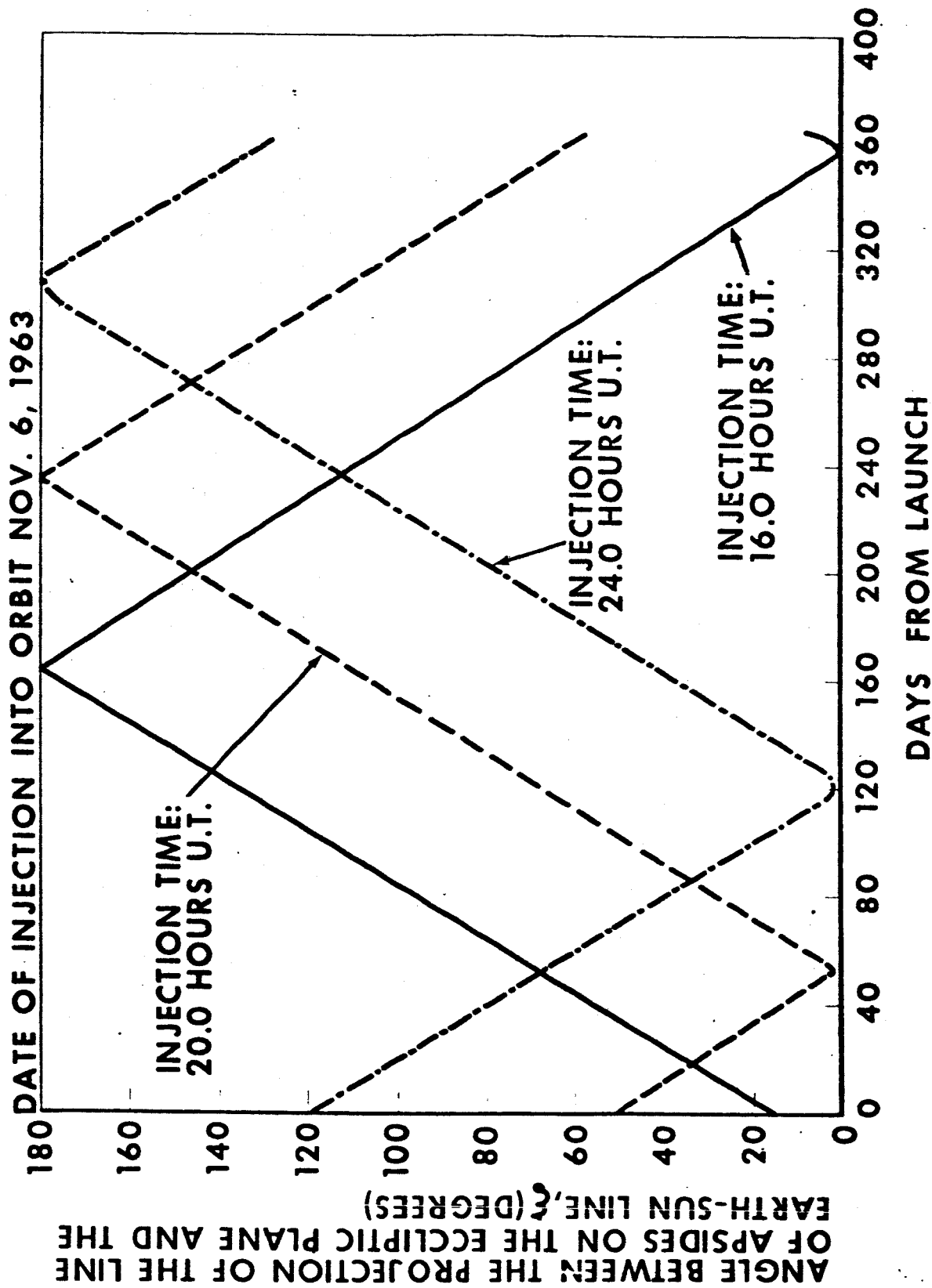


Figure 15. Angle between the projection of the line of apsides on the ecliptic plane and the earth-sun line.

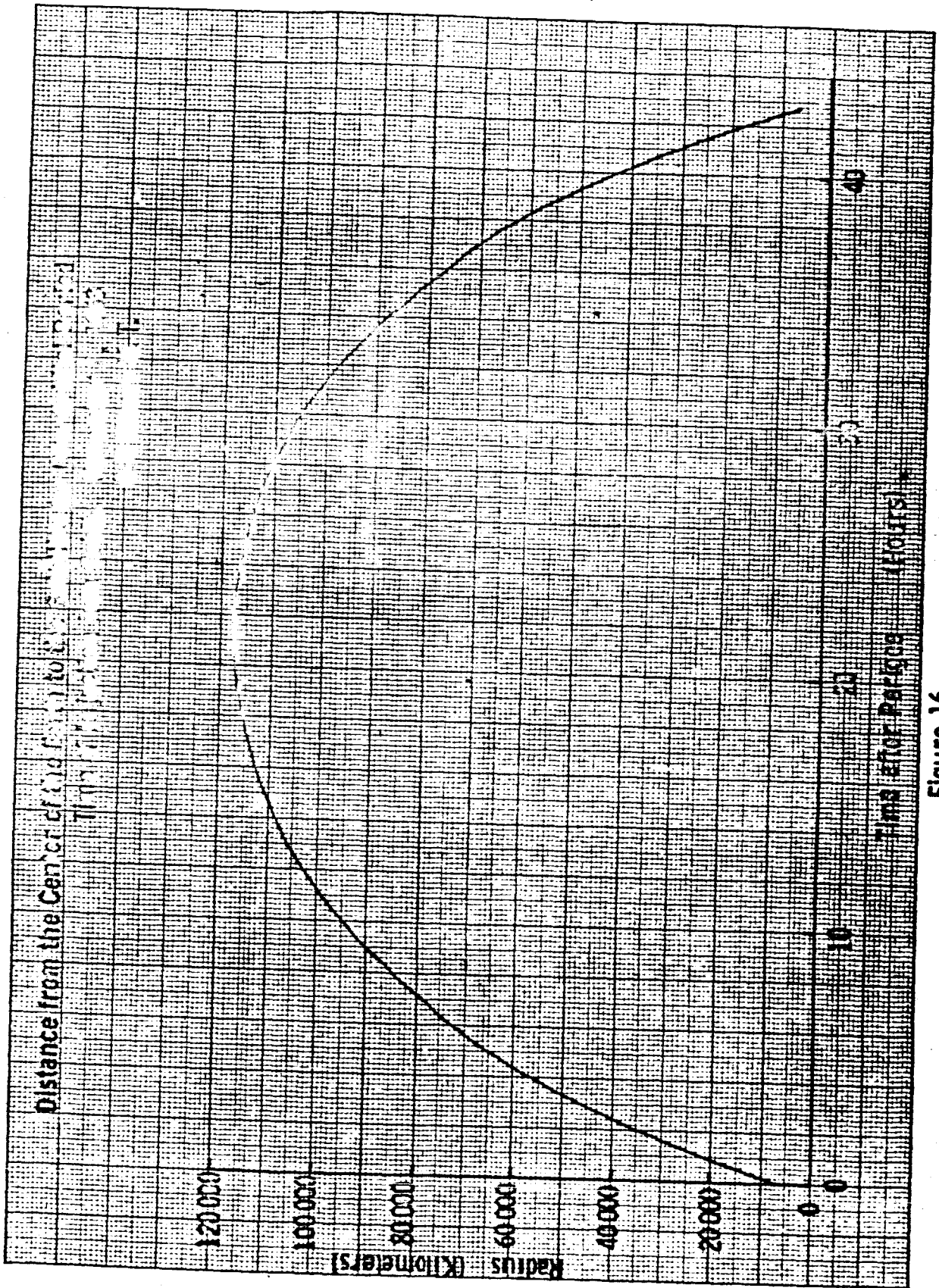


Figure 16

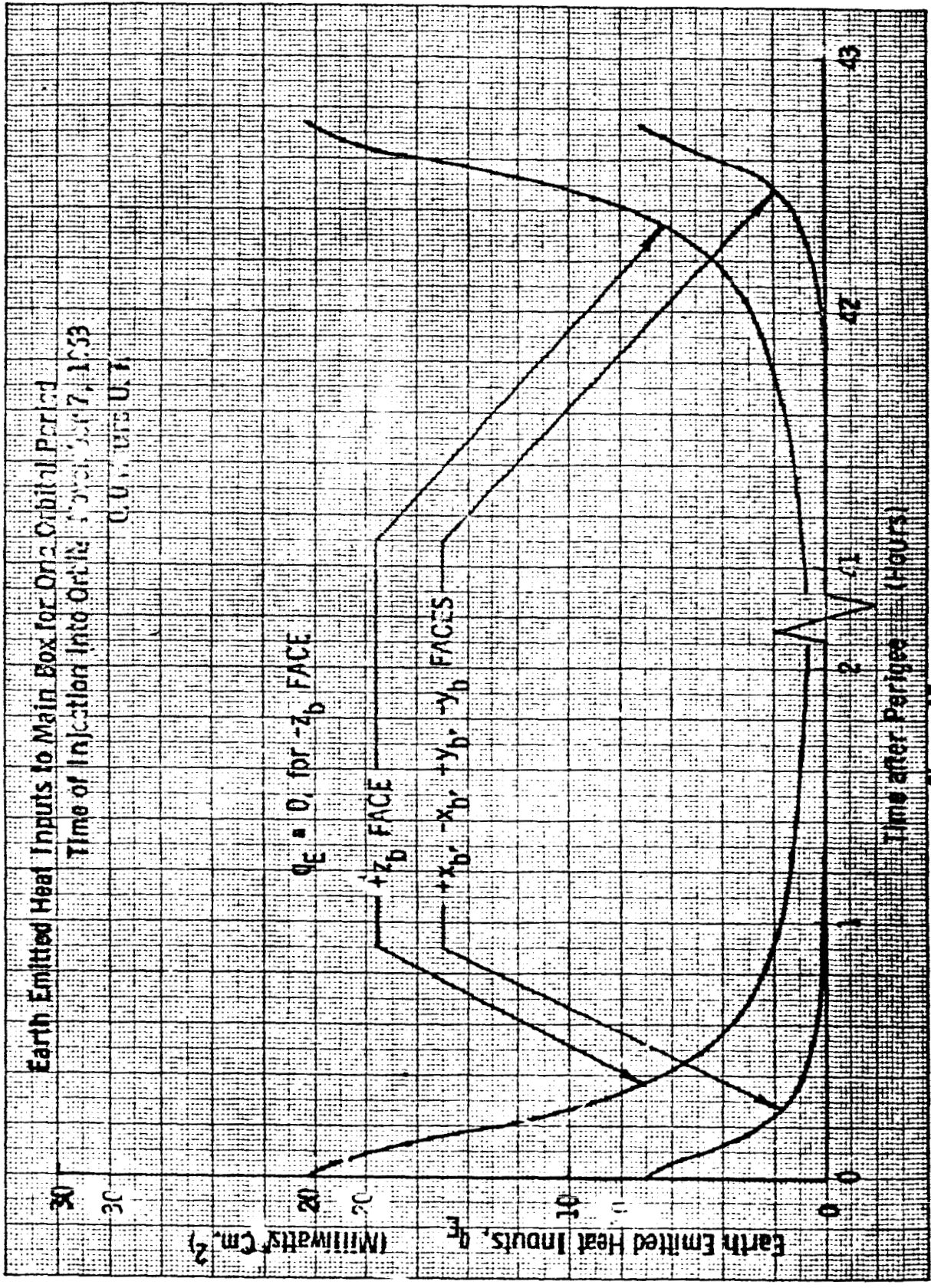


Figure 17

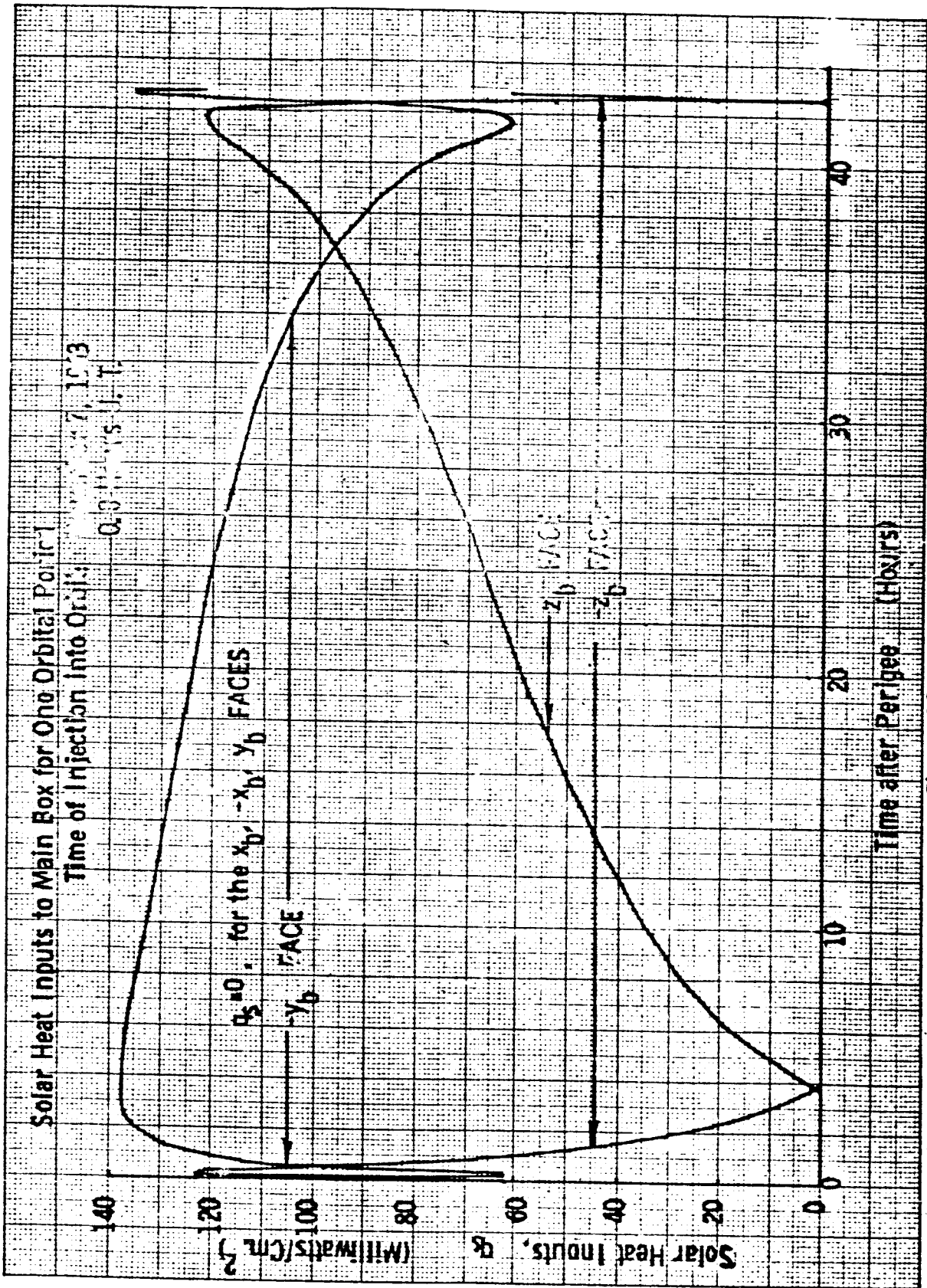


Figure 18

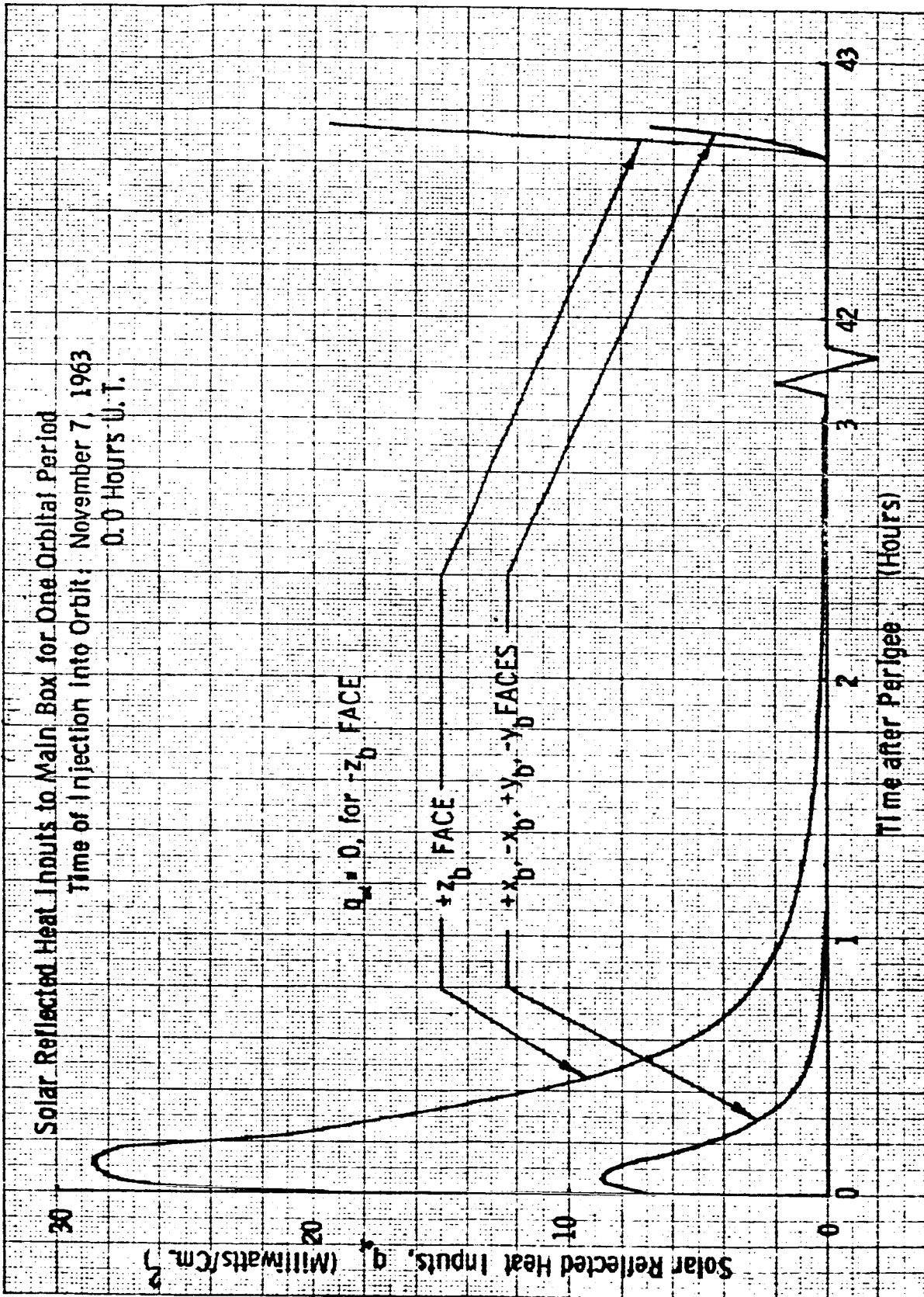


Figure 19

Earth Emitted Heat Inputs to Solar Array For One Orbital Period.  
 Time of Injection into Orbit: November 7, 1963  
 0.0 hours U. T.

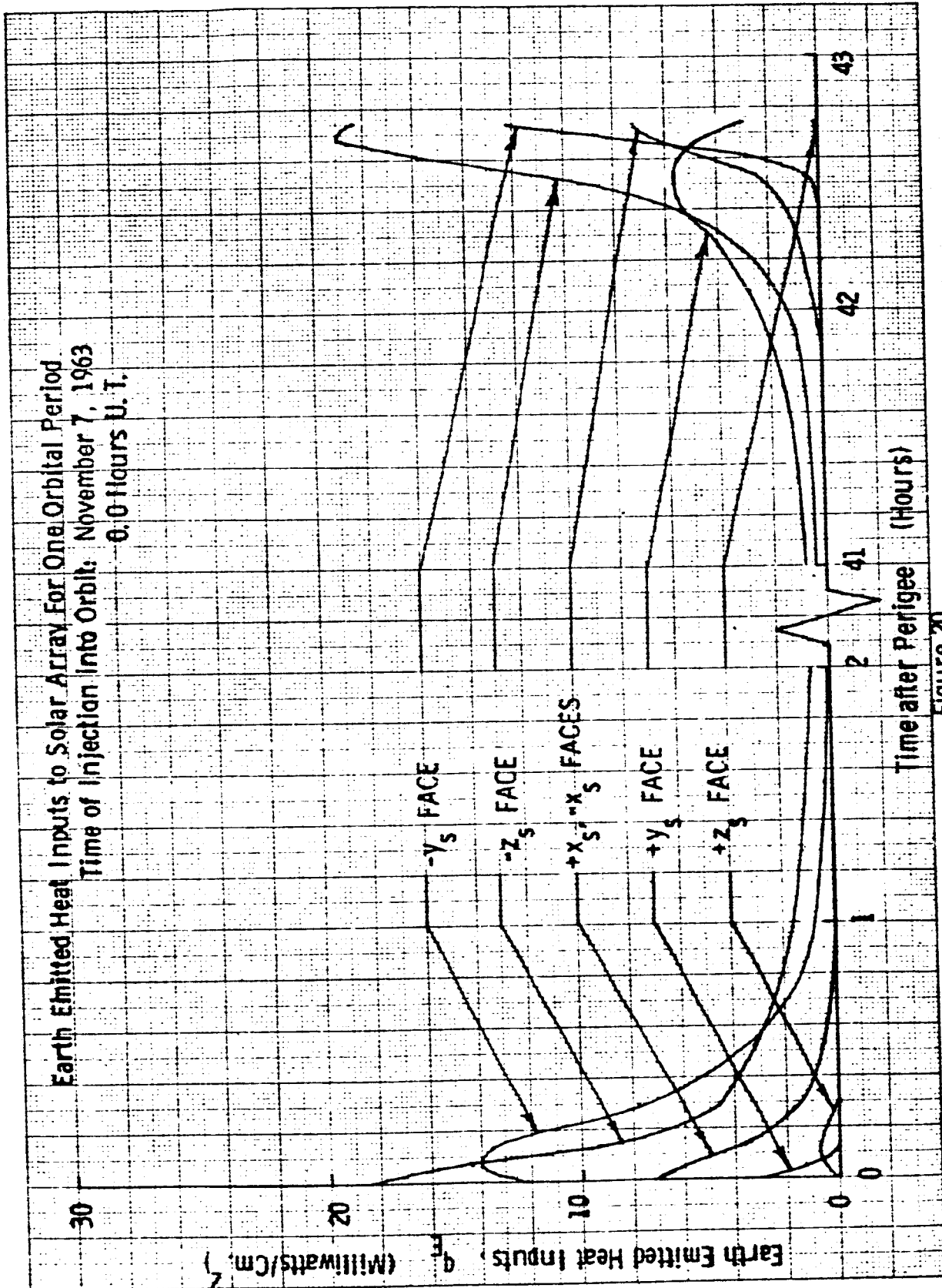


Figure 20

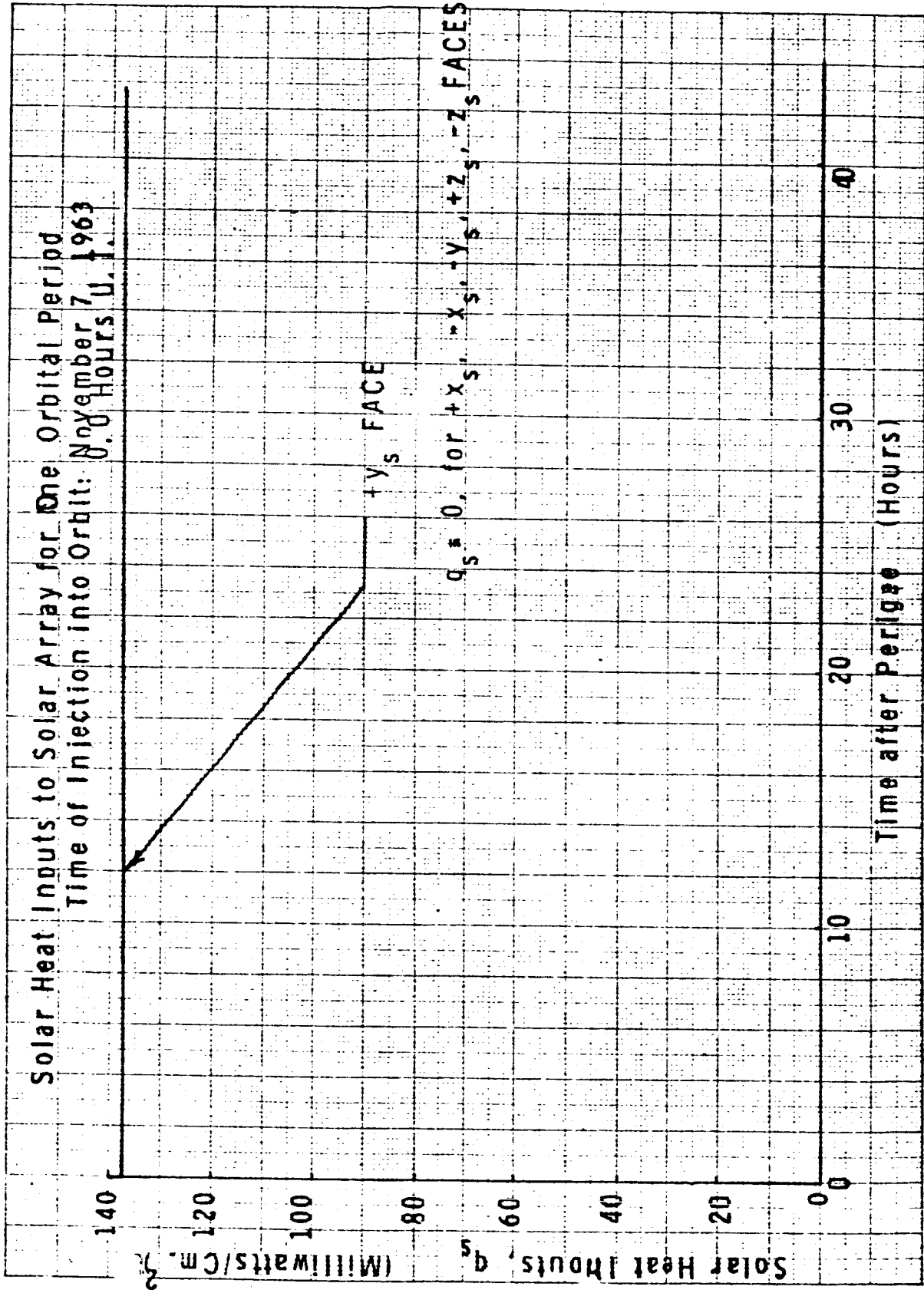


Figure 21

Solar Reflected Heat Inputs to Solar Array for One Orbital Period  
 Time of Injection into Orbit: November 7, 1963  
 0:0 Hours U.T.

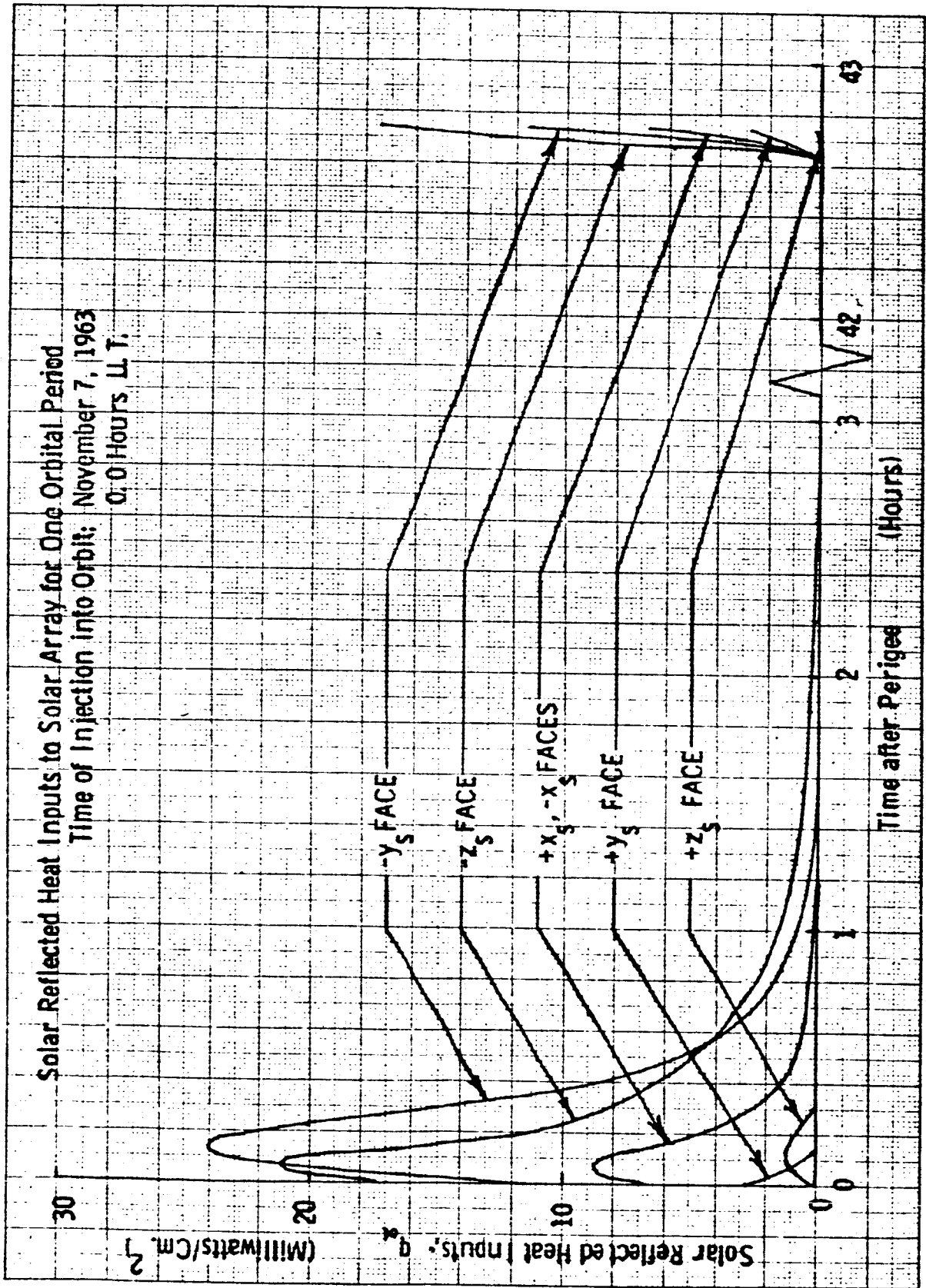


Figure 22

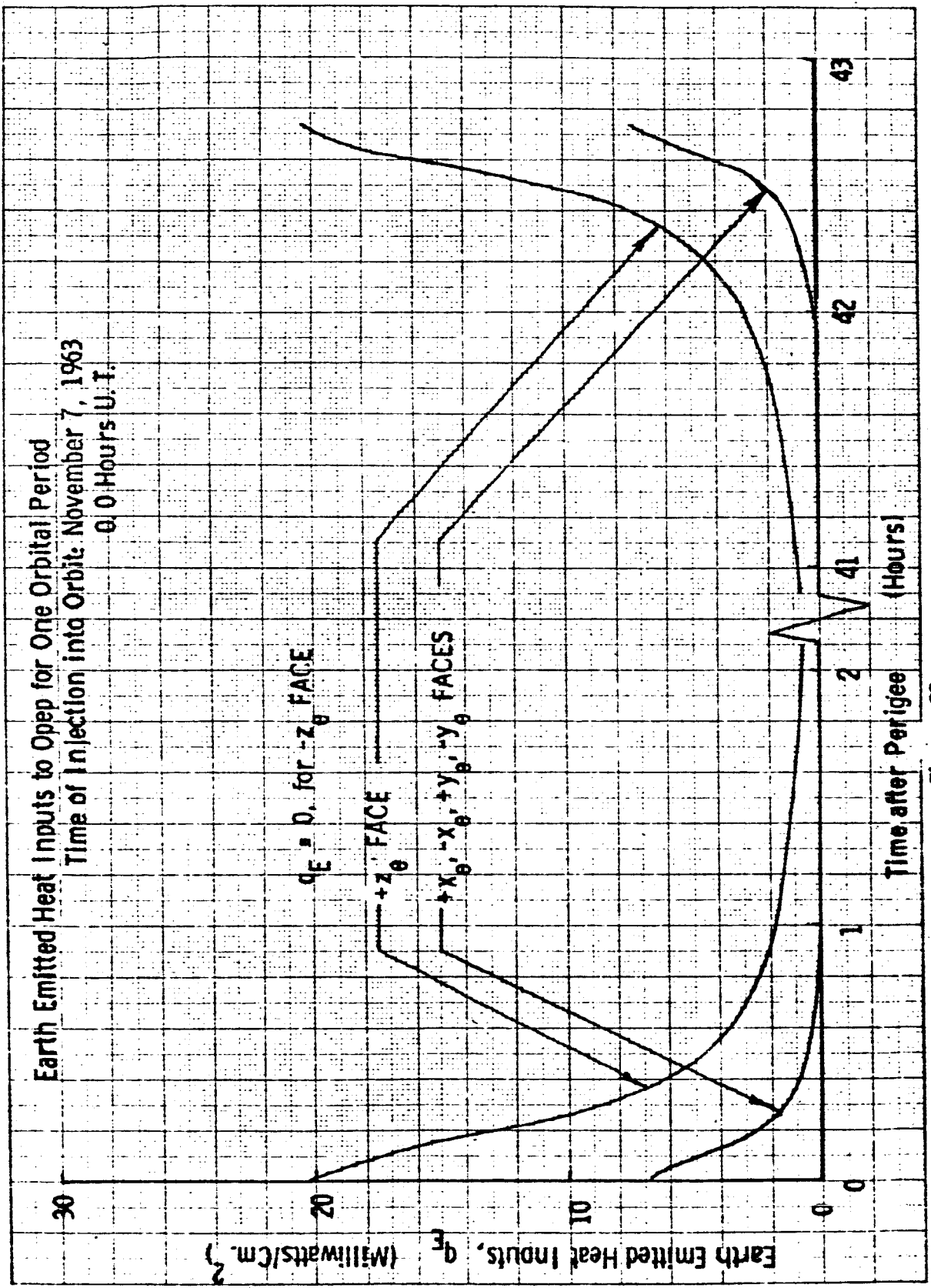


Figure 23

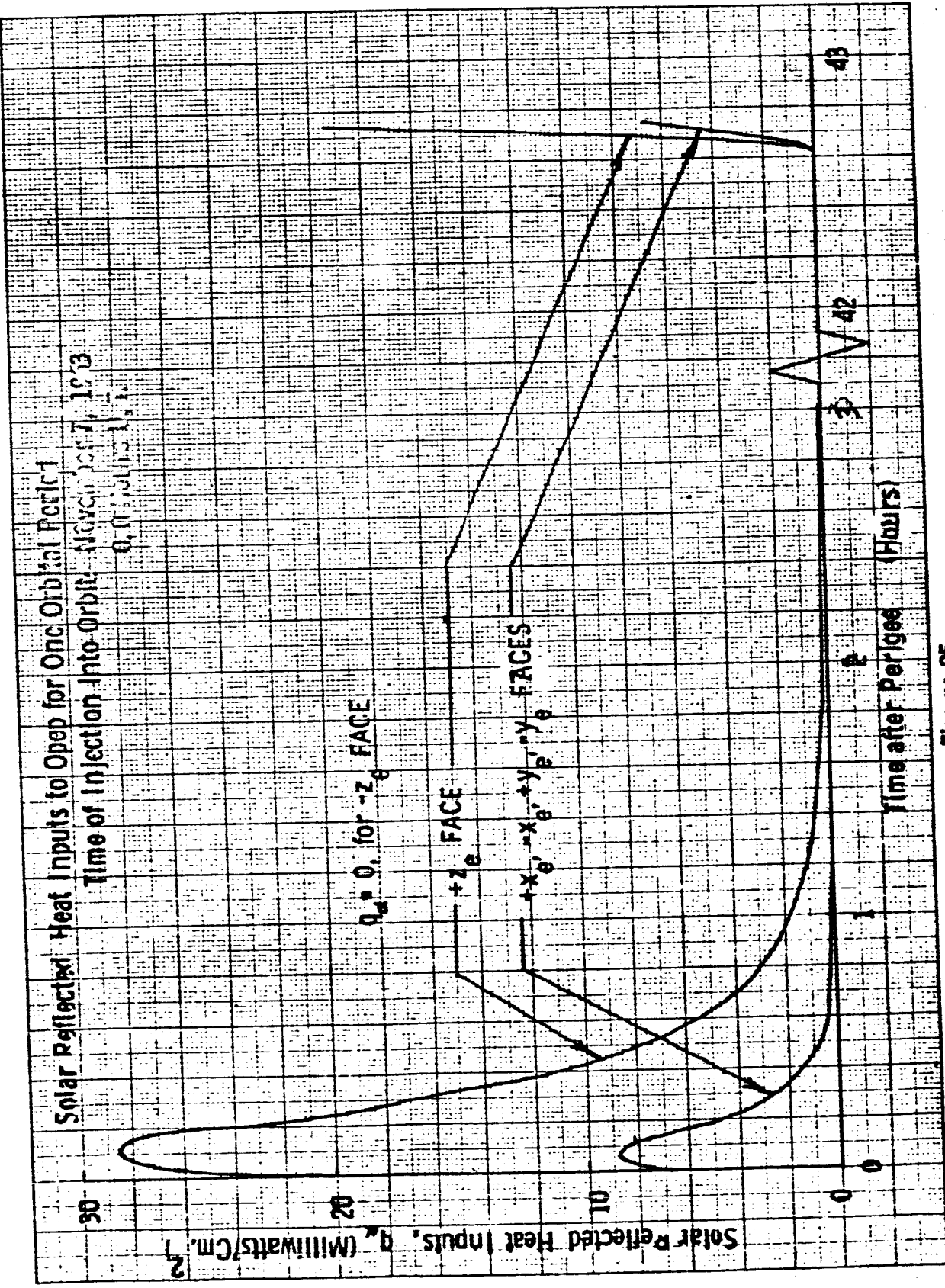


Figure 25